ESD-TR-69-338

Technical Report 470

E. J. Denlinger

Dynamic Solutions for Single and Coupled Microstrip Lines

19 November 1969

Prepared for the Office of the Chief of Research and Development, Department of the Army, under Electronic Systems Division Contract AF 19(628)-5167 by

Lincoln Laboratory

MASSACHUSETTS INSTITUTE OF TECHNOLOGY

Lexington, Massachusetts

MASSACHUSETTS INSTITUTE OF TECHNOLOGY

LINCOLN LABORATORY

DYNAMIC SOLUTIONS FOR SINGLE AND COUPLED MICROSTRIP LINES

E. J. DENLINGER

Group 34

TECHNICAL REPORT 470

19 NOVEMBER 1969

LEXINGTON MASSACHUSETTS

The work reported in this document was performed at Lincoln Laboratory, a center for research operated by Massachusetts Institute of Technology. The work is sponsored by the Office of the Chief of Research and Development, Department of the Army; it is supported by the Advanced Ballistic Missile Defense Agency under Air Force Contract AF 19(628)-5167.

DYNAMIC SOLUTIONS
FOR SINGLE AND COUPLED MICROSTRIP LINES*

ABSTRACT

This investigation presents theoretical and experimental results of single and coupled microstrip propagation on both a pure dielectric and a ferrite substrate. The theory enables one to obtain the frequency dependence of phase velocity and characteristic impedance and also to obtain the electromagnetic field quantities around the microstrip line. It utilizes a Fourier transform method in which the hybrid mode solutions for a "fictitious" surface current at the substrate-air interface are summed in such a way as to represent the fields caused by a current distribution that is finite only over the region occupied by the conducting strip and is assumed equal to that for the static case. The theory for the magnetized ferrite microstrip takes into account both the diagonal and off-diagonal components of the substrate's permeability tensor.

Excellent agreement is obtained between experimental and theoretical results for single microstrip lines on both ceramic and demagnetized ferrite substrates. Coupled line experimental data also agree well with theory and show a significant difference in the amount of dispersion of the two normal modes of propagation, the even mode and the odd mode.

The coupled microstrip theory is then applied to two commonly used microwave integrated circuit devices, the directional coupler and the meander-line phase shifter. Since the even- and odd-mode phase velocities for ferrite-filled coupled lines are closer together than those for the pure dielectric case, the coupler performance with ferrite is shown to be significantly better than with ceramic. Theoretical results which illustrate the nonreciprocal character of the meander-line's propagation constants are also presented.

Accepted for the Air Force
Franklin C. Hudson
Chief, Lincoln Laboratory Office

---

* This report is based on a thesis of the same title submitted to the faculty of the Graduate School of Arts and Sciences of the University of Pennsylvania on 1 December 1969, in partial fulfillment of the requirements for the degree of Doctor of Philosophy.

CONTENTS

PREFACE

For nearly seventeen years, microstrip transmission lines have been the subject of considerable theoretical and experimental investigation. They are extensively used today in microwave integrated circuits because of their relative ease of fabrication by the use of printed circuit techniques. Up to the present time, their properties have been predicted assuming that they support a quasi-TEM mode. Various electrostatic approximations have been quite useful at low frequencies for the design of microstrip circuits. However, the fact which has been neglected is that the actual propagating modes cannot be TEM because of the presence of an air-dielectric interface. In reality, there are components of both electric and magnetic fields in the direction of propagation.

A very important configuration that is an inherent part of such devices as directional couplers, phase shifters, filters, etc., is a coupled pair of microstrip lines. In order to adequately predict the performance of these devices in terms of cutoff frequencies, bandwidth, etc., it would be advantageous to have a frequency-dependent solution of the coupled strip's propagation characteristics. This is particularly true when it is desirable to increase the power-handling capability by making the microstrip substrate thicker. The amount of dispersion is largely dependent upon the latter parameter.

In this report, a solution is presented that will predict the dynamic behavior of single and coupled microstrip on both dielectric and ferrite substrates. It is a hybrid mode solution that accounts for the longitudinal components of the fields as well as the dielectric discontinuity of an open microstrip line. From the following theoretical and experimental results, more flexibility in choosing microstrip parameters, such as the substrate's material, dielectric constant, and thickness, should facilitate the attainment of the desired frequency characteristics of microstrip circuit components.

DYNAMIC SOLUTIONS FOR SINGLE AND COUPLED MICROSTRIP LINES

I. INTRODUCTION

The major objective of this dissertation is to give a dynamic (frequency-dependent) solution for both a single microstrip line and a coupled pair of microstrip lines. A microstrip is a two-conductor transmission line consisting of a narrow conducting strip deposited onto a thin substrate which has its other side entirely coated with a conducting ground plane. The substrate materials that will be considered here are either a pure dielectric material, such as rutile, alumina, magnesium titanate, teflon quartz, etc., or a gyromagnetic material such as a ferrite, which is sometimes magnetized along the direction of propagation. This type of transmission line is very attractive, particularly in connection with microwave integrated circuit applications involving a large number of identical units and requiring a high density of packaging such as in phased-array radar where devices involving both single and coupled microstrip lines are used. These include transmission lines and matching networks in receiver amplifier circuits, directional couplers, band-pass filters, and nonreciprocal devices such as circulators, isolators, and meander-line phase shifters.

Since the microstrip structure is unsymmetrical, an exact solution for the transmission line parameters such as phase velocity, characteristic impedance, etc., is very complicated. For this reason, nearly all the numerical solutions obtained thus far have been quasi-static approximations which assume a TEM mode of propagation.

The first extensive study of microstrip lines for propagation of microwave energy was published nearly seventeen years ago by Assadourian and Rimai.[1] Their approximate analysis involving conformal mapping provided useful design equations for ratios of strip width to substrate thickness much greater than unity.

In 1954, Deschamps[2] discussed the possible modes of propagation on a microstrip line. He pointed out that no pure TE or TM mode solutions are possible and that the existence of at least one surface-wave mode resulting from the perturbation by the dielectric of the fundamental TEM mode can be assumed. During that same year, Schetzen[3] obtained a TE-TM mode solution by assuming a longitudinal component of current having a constant amplitude across the width of the strip. This led him to the false conclusion that the phase velocity is constant with frequency.

In 1955, Black and Higgins[4] derived in a lengthy analysis an expression for the capacitance per unit length of line.

The main difficulty in obtaining a complete solution stems from the necessity of taking into account the dielectric discontinuity at the insulator boundary, the fringe fields, the finite conductor size, and the radiation loss. The approximate theories, which are based on TEM propagation, account for the fringing fields but neglect the dielectric discontinuity and the radiation.

Wu[5] tried to account for some of these effects by formulating a pair of coupled integral equations for the two unknown components of current density that exist on the strip, namely the longitudinal component I_z and the transverse component I_x. However, because of the extreme complexity of these equations, they have never been solved.

In 1958, Brodwin[6] used Van Trier's analysis[7] of a ferrite-filled parallel plane waveguide as an approximation to a ferrite-filled microstrip line having a strip width of at least a half-wavelength. A simple relationship was obtained between the propagation constant and the applied longitudinal magnetic field for a quasi-TEM mode.

Wheeler[8,9] published a conformal mapping analysis of TEM propagation on a dielectric-filled microstrip line which does account for the dielectric discontinuity. His calculations show fairly good correlation with low-frequency experimental measurements for all lines, including those with width-to-substrate thickness ratios less than unity.

Green[10] presented a generalized numerical solution of Laplace's equation in two dimensions for determining the characteristic impedance and propagation constant of TEM-mode transmission lines. He applied his method to a microstrip line by imagining the latter to be enclosed in a conducting screen of dimensions large compared with the cross section of the line. This is an approximation of the boundary condition that the potential at infinity is zero.

Caulton, Hughes, and Sobol[11] used Wheeler's conformal mapping theory to derive in 1966 a set of design curves for microstrip lines applicable over a wide range of geometries and substrate materials. Design data was presented for characteristic impedance, wavelength, attenuation, and line width correction for finite-thickness conductors.

Silvester[12] used the classical method of images as well as the Green's function solution for a pair of unit charges separated by a dielectric sheet to obtain a Fredholm integral equation for the unknown charge distribution on the strip. Hence, the electrostatic capacitance per unit length of the microstrip line can be determined along with the velocity of propagation and the characteristic impedance.

A variational method was used by Yamashita[13,14] to calculate the microstrip line capacitance and guide wavelength. This method is based on a variational calculation of the line capacitance in the Fourier-transformed domain and on the charge density distribution as a trial function.

Hartwig, Massé, and Pucel[15] qualitatively described the frequency-dependent behavior of microstrip. As was earlier pointed out by Deschamps, there exist surface-wave modes which couple to the TEM mode. The two lowest order modes are the TM_0, which has a zero frequency cutoff and the TE_1, which has a finite cutoff frequency, below which it cannot exist. Above this frequency f_c, determined by the dielectric constant and thickness of the substrate, it was experimentally found that the energy cannot be confined to the microstrip line. In fact, energy will propagate on the substrate and radiate from its edges.

A theoretical analysis of both a single microstrip line and a coupled pair of lines was published by Bryant and Weiss.[16] The discontinuity of the fields at the dielectric-vacuum interface was expressed by a "dielectric Green's function." In a manner similar to Silvester's method, the capacitance for the single and coupled strips was determined from the charge distribution, which was the solution of a Fredholm integral equation. Then the velocity of propagation and the characteristic impedance were obtained using quasi-static approximations.

Recently, there have been solutions for a microstrip line bounded by a metal "box" with dimensions large compared with the width of the strip and the substrate thickness. For this

case, the boundary conditions are confined to a finite cross sectional area. Stinehelfer[17] used a relaxation technique similar to that accomplished by Green for computing the solution of Laplace's equation. A hybrid mode solution giving the frequency dependence of the guide wavelength was obtained by Zysman and Varon.[18] In this analysis, the hybrid modes were decomposed into sums of LSE and LSM† space harmonics, each satisfying the wave equation for an inhomogeneously filled waveguide without the center conductor, and their total satisfying the continuity conditions and boundary conditions on the strip.

Today there is great need for a dynamic solution for open microstrip propagation. In the early days, this type of transmission line was abandoned in favor of the balanced-strip transmission line because of the radiative nature of the open-strip line. However, the recent availability of low loss, high-dielectric-constant materials made possible a great reduction of the radiation from microstrip. As a result, this line has recently been actively used for integrated microwave printed circuits. Even though a higher dielectric-constant substrate reduces the radiation, it also increases the amount of dispersion of the microstrip's parameters. In addition, much effort is being placed on increasing the power-handling capability of microstrip circuits, which might include such devices as circulators and phase shifters. This requires a reasonably thick substrate which again, as shown in Sec. V, increases the amount of dispersion. Since microwave integrated circuits are being used frequently anywhere from 1 through 12 GHz, and even higher in some cases, the resulting amount of dispersion, while taking account of such factors as radiation and power-handling capability, results in TEM solutions which are no longer very good approximations.

This report presents a solution that will give the frequency dependence of phase velocity and characteristic impedance for both a single microstrip line and a coupled pair of lines. Four different situations pertaining to the substrate material are treated: (1) a pure dielectric substrate; (2) a demagnetized ferrite substrate; (3) a magnetized ferrite substrate; and (4) a magnetized ferrite substrate with the RF magnetic fields assumed to be circularly polarized. In Sec. II, the theory for a single microstrip line on both a pure dielectric substrate and a demagnetized ferrite substrate is given. Two different solutions for the electromagnetic fields and the microstrip phase velocity are presented: one assumes the presence of both a longitudinal and a transverse component of current on the center conductor (or strip); the other assumes the existence of only a longitudinal current. The latter solution is much simpler and is proven to be an excellent approximation. An equation for the characteristic impedance is then derived in terms of the field expressions and the phase velocity. Section III is devoted to the theory for a ferrite-filled microstrip line which is magnetized along the direction of propagation. Since the ferrite permeability is a tensor quantity, a large number of symmetrical and unsymmetrical propagating modes can exist. Section IV shows that a simple extension of the above two theories is required to solve the coupled microstrip problem. Expressions for the phase velocity and the characteristic impedance are derived for the two normal modes of propagation, which are known as the even and odd modes. Application of this theory is made to two microstrip devices: the quarter-wave directional coupler and the meander-line phase shifter. In Sec. V the theoretical equations presented in the previous sections are applied to typical microstrip cases by numerical computation on an IBM 360 digital computer situated at Lincoln Laboratory. A comparison with experimental results is included for both dielectric and ferrite-filled microstrip. In all the work described in this report, the mks system of units is used whenever possible.

† LSE refers to a mode which has na electric field component normal to the substrate-air interface; an LSM mode has no magnetic field component normal to the interface.

II. THEORY FOR MICROSTRIP ON A PURE DIELECTRIC OR ON A DEMAGNETIZED FERRITE SUBSTRATE

A. Introduction

As outlined in the previous chapter, Wheeler,[9] Bryant and Weiss,[16] and others have obtained quasi-static solutions of the microstrip problem which are applicable only in the low-frequency range where the propagation may be regarded as approximately TEM. However, Hartwig, et al.,[15] and Welch[19] have found that the microstrip line is quite dispersive at elevated frequencies due to coupling between the so-called TEM Wheeler mode and the two lowest-order surface-wave modes (TM_0 and the TE_1 modes). The object of this section is to present a TE-TM mode solution which gives the frequency dependence of microstrip propagation on a pure dielectric substrate or a demagnetized ferrite substrate, both of which are assumed to be completely lossless.

Figure 1 shows the physical construction of the microstrip line, which can be described as a narrow conducting strip deposited by printed circuit techniques onto a thin, flat substrate that has its other side entirely coated with a conducting ground plane. Both the substrate and the ground plane are infinite in extent. The configuration is conventionally specified by the parameters w/d and K for a ceramic substrate and an additional parameter μ_r for a ferrite substrate; w is the strip width, d is the substrate thickness, K is the relative dielectric constant, and μ_r is the relative ferrite permeability. The latter two parameters are considered to be purely scalar quantities, which is true for both a ceramic substrate and a demagnetized ferrite substrate. As shown later, μ_r is frequency-dependent and is a function of the ferrite material's saturation magnetization. In this analysis, the strip is assumed to have a negligibly small thickness and both strip and ground plane are assumed to have infinite conductivity. Given the values of the parameters defined above, the theory enables one to obtain the phase velocity, the effective dielectric constant, and the effective permeability as a function of frequency. Also, the characteristic impedance of the microstrip line can be calculated using a quasi-static definition.

The formulation of an exact theory for the microstrip structure is difficult because the cross section is not homogeneous. Furthermore, microstrip is an open structure where the energy is not confined to a finite region. Without the dielectric, it would be a Lecher-type structure that

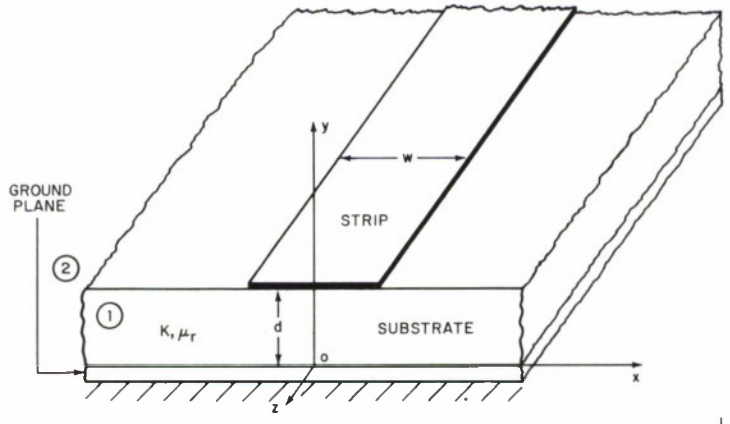

Fig. 1. Microstrip configuration.

could support a TEM mode. However, the presence of the dielectric causes the refractive index to vary over the cross section; therefore, the wave can be TEM only at zero frequency. For a simple grounded dielectric slab configuration subject to a physical field due to some arbitrary source, the complete solution consists of a discrete number of surface waves, a continuous spectrum of evanescent waves, and a continuous eigenvalue field, i.e., radiation field.[20] Leaky modes which correspond to a flow of power away from the surface do not satisfy the radiation conditions at infinity and thus do not belong to the proper eigenvalue spectrum. They are only used to partially represent the radiated field from some elementary source.[21] In the following theory for microstrip, the sources for the electromagnetic field are assumed to be located at infinity so that the only free propagation modes that are considered to exist are surface wave modes and the TEM mode. Due to boundary conditions involving transverse inhomogeneity in the dielectric and the presence of the strip, no pure TEM, TE, or TM modes may exist.[2] Thus, a hybrid mode solution that can be expressed in terms of a complete set of simpler solutions having a z-dependence of e^{-jkz} is sought. The proof of mode orthogonality for surface waveguides, as presented by Collin,[21] enables a given arbitrary field to be expanded into a series of TE and TM modes. A linear combination of these modes is allowed for the case where the substrate's permeability and dielectric constant are both scalar quantities. The following gives the derivation of a hybrid TE-TM mode of propagation.

B. Derivation of Electromagnetic Field Expressions

Two different analyses are presented here: one takes into account the presence of both a longitudinal and a transverse component of current on the strip; the other is more of a quasi-static solution which assumes that only a longitudinal current exists.

1. Analysis for Both Longitudinal and Transverse Currents

The method of solution is to construct series of functions, each of which independently satisfies the wave equation for a TE mode or a TM mode and also satisfies boundary conditions on the ground plane and at infinity. Appropriate sets of functions are obtained by taking a Fourier transform of the fields along the x-axis, which is oriented as shown in Fig. 1. The remaining boundary conditions on the strip and along the substrate-air interface are satisfied by the use of a linear combination of the TE mode and TM mode fields. A solution for the Fourier components of the fields is first obtained for a grounded dielectric (or ferrite) slab which does not possess a current carrying strip. Instead, it has a "fictitious" surface current whose amplitude varies sinusoidally in the x direction along the substrate-air interface and has vector components both in the x- and the z-directions. The hybrid mode fields that are caused by the actual current distribution, which is nonzero only over the region occupied by the strip, are found by taking a Fourier integral of the above sinusoidal components and are forced to satisfy the requirement that the tangential electric field vanish on the strip.

The Fourier transform method described above was used by Schetzen[3] in 1954 to obtain the fields which result from a uniform longitudinal current distribution on the strip. His theoretical analysis of a microstrip line on a pure dielectric substrate resulted in the invalid conclusion that the phase velocity is constant with frequency. From the Green's function static solution of Bryant and Weiss,[16] it is clear that the current is not constant across the strip width. In fact, its amplitude increases very rapidly at the edges of the strip. Therefore, a more valid longitudinal current distribution can be obtained from the following relationship for the charge density

TABLE II-1

CURRENT DISTRIBUTION DATA – COMPARISON OF GREEN'S FUNCTION SOLUTION WITH THAT USING MAXWELL'S FUNCTION [Eq. (2-1)]
[m = number of elementary strip widths
($\Delta x/d = 0.025$) from center of strip region (x = 0)]

m	I(m): K = 1; w/d = 0.5		I(m): K = 15; w/d = 0.5	
	Maxwell's Function	Green's Function	Maxwell's Function	Green's Function
1	0.5843	0.5836	0.5481 × 10	0.5474 × 10
2	0.5903	0.5895	0.5537	0.5529
3	0.6027	0.6020	0.5653	0.5644
4	0.6230	0.6223	0.5844	0.5831
5	0.6535	0.6530	0.6130	0.6115
6	0.6988	0.6989	0.6555	0.6539
7	0.7680	0.7692	0.7204	0.7190
8	0.8823	0.8893	0.8276	0.8302
9	1.1078	1.0800	1.0391	1.0070
10	1.8690	2.4490	1.7531	2.2800

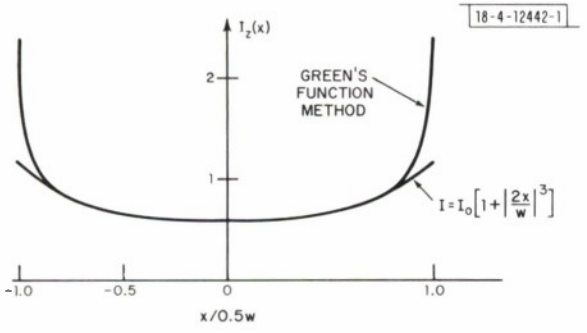

Fig. 2. Longitudinal current distribution on microstrip.

distribution on an isolated conducting strip[22,23] (see Appendix A for derivation):

$$\sigma(x) = \frac{\sigma_o}{\pi\sqrt{1-(2x/w)^2}} \qquad -w/2 < x < w/2$$

$$= 0 \quad \text{otherwise} \quad . \tag{2-1}$$

For the dynamic case, the current is simply $I_z(x) \cong v\sigma(x)$, where v is the phase velocity. This relationship agrees extremely well with the current distribution obtained from the Green's function solution.[16] Table II-1 illustrates this agreement by giving the computed data for two widely different substrate dielectric constants. It was also found that changing the w/d ratio between 0.2 and 1.2 only affected the amplitude σ_o without changing the current's functional dependence on x. In the analysis to follow, the Fourier transform of $I_z(x)$ is made use of. Therefore, the value of σ_o is not needed in order to find the desired quantities of phase velocity and characteristic impedance. The Fourier transform of the current distribution is given by a zero order Bessel function, which can be expanded into an infinite series in terms of the Fourier transform variable α:

$$I_z(\alpha) = \frac{1}{2\pi}\int_{-\infty}^{\infty} I_z(x)\, e^{-j\alpha x} dx$$

$$= \frac{w}{2}\, I_{zo} J_o(\alpha w/2) \quad .$$

In series form

$$I_z(\alpha) = \frac{w}{2}\, I_{zo} \sum_{m=0}^{\infty} \frac{(-1)^m (\alpha w/4)^{2m}}{(m!)^2} \tag{2-2}$$

where

$$I_{zo} \cong v\sigma_o \quad .$$

It will be shown in Sec. V that the use of this current function gives results that are in excellent agreement with experimental results and with the TEM solutions at zero frequency. However, the computations require excessive computer time. Another expression given by Eq. (2-3) was found to give sufficient accuracy and yet its Fourier transform allowed the computer time to be reduced by a factor of five (from two minutes to about twenty-four seconds per point):

$$I_z(x) = I_{zo}(1 + |2x/w|^3) \qquad |x| \leq w/2$$

$$= 0 \quad \text{otherwise} \quad . \tag{2-3}$$

The Fourier transform of Eq. (2-3) is

$$I_z(\alpha) = \frac{2I_{zo}}{\pi\alpha}\left\{\frac{24}{(\alpha w)^3} + \frac{3[(\alpha w)^2 - 8]}{(\alpha w)^3}\cos(\alpha w/2) + \frac{(\alpha w)^2 - 12}{(\alpha w)^2}\sin(\alpha w/2)\right\} \quad . \tag{2-4}$$

Figure 2 shows a comparison between the current distribution given by the above function and that calculated by the Green's function method. The effect of the lower $I_z(x)$ near the edge of the

strip is to give a slightly lower value (less than 1 percent) for the microstrip line's effective dielectric constant.

In order to estimate the transverse component of current, the continuity equation is utilized to relate this quantity to the charge density distribution $\sigma(x)$ on the strip in the following manner (see Appendix A):

$$\frac{dI_x(x)}{dx} = -j\omega\sigma(x) \tag{2-5}$$

where ω = angular frequency. Substituting an expression of the same form as Eq. (2-1) for $\sigma(x)$ and solving for the current gives

$$I_x(x) = -j\,\frac{\omega\sigma_o}{\pi}\,\frac{w}{2}\,\sin^{-1}\left(\frac{2x}{w}\right) \qquad -w/2 < x < w/2$$

$$= 0 \quad \text{otherwise} \quad . \tag{2-6}$$

Figure 3 shows the form of this current distribution across the width of the strip. Taking the Fourier transform results in

$$I_x(\alpha) = -\frac{1}{4}\,\omega\sigma_o w^2\,\frac{J_o(\alpha w/2)}{\alpha w/2} \quad . \tag{2-7}$$

The electromagnetic field expressions to be derived are exact for the case of a sinusoidal surface current distribution flowing along the substrate-air interface which does not possess a conducting strip. However, the solutions for an infinite number of these "fictitious" sinusoidal

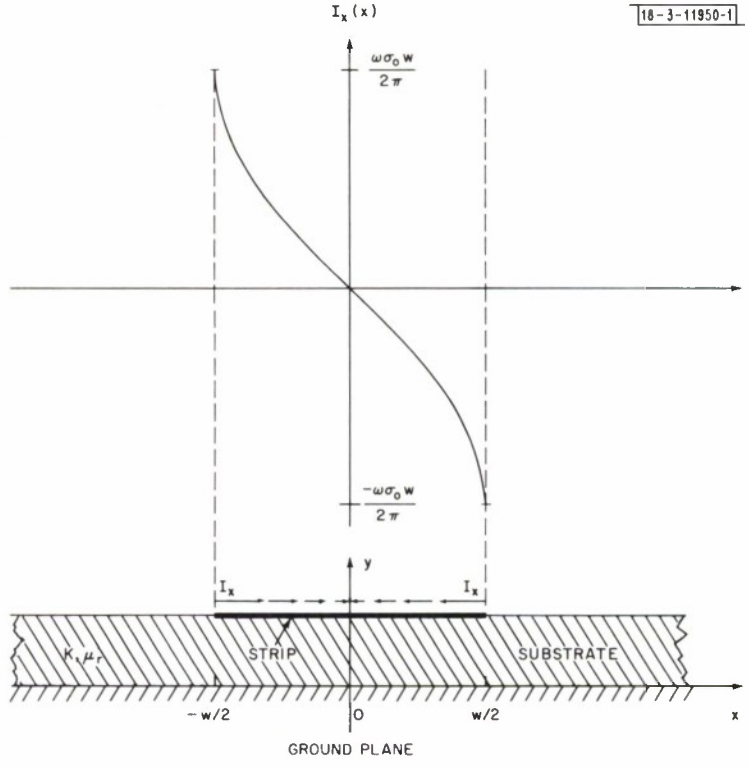

Fig. 3. Transverse current distribution on microstrip.

components are summed up in such a manner as to represent the fields caused by a current distribution that is finite only over the strip width w and equal to the static charge distribution. At this stage, the "conducting" strip is simply represented by a surface current over a finite region w. The introduction of the boundary condition that the tangential electric field be zero at (y = d), $|x| \leq w/2$) results from the strip being a perfect conductor.

The "fictitious" surface current flowing at the substrate-air interface generates a hybrid TM-TE mode, which can be represented as a linear combination of TM and TE modes because these modes form a complete set in terms of which an arbitrary field can be represented. For a cylindrical structure of arbitrary cross section, the TM and TE modes may be derived from an electric-type Hertzian potential $\bar{\pi}_e = \bar{a}_z N\psi_e(x, y)\, e^{j(\omega t - kz)}$ and a magnetic Hertzian potential $\bar{\pi}_h = \bar{a}_z N\psi_h(x, y)\, e^{j(\omega t - kz)}$, respectively.[24] N is an arbitrary constant that is dependent upon the source strength while the functions ψ_e and ψ_h both satisfy a two-dimensional scalar Helmholtz equation given below.

$$\nabla_t^2 \psi_{e,h} + \nu^2 \psi_{e,h} = 0 \tag{2-8}$$

where

$$\nu^2 = \begin{cases} P_1^2 = \omega^2 \mu_r K \mu_o \epsilon_o - k^2 & y < d \\ P_2^2 = \omega^2 \mu_o \epsilon_o - k^2 & y > d \end{cases} .$$

Regions 1 and 2 are the substrate and air regions, respectively. The above potential functions can be written in terms of their Fourier transform $\psi(\alpha, y)$ with respect to x,

$$\psi(x, y) = \frac{1}{2\pi} \int_{-\infty}^{\infty} \psi(\alpha, y)\, e^{j\alpha x} d\alpha \quad . \tag{2-9}$$

Combining Eqs. (2-8) and (2-9) results in the following differential equations:

$$\left(\frac{d^2}{dy^2} + P_2^2 - \alpha^2\right) \begin{Bmatrix} \psi_e(\alpha, y) \\ \psi_h(\alpha, y) \end{Bmatrix} = 0 \qquad y > d$$

and

$$\left(\frac{d^2}{dy^2} + P_1^2 - \alpha^2\right) \begin{Bmatrix} \psi_e(\alpha, y) \\ \psi_h(\alpha, y) \end{Bmatrix} = 0 \qquad y < d \quad . \tag{2-10}$$

Since the total energy of the wave must be finite and the natural propagating modes for the grounded dielectric slab configuration are surface modes,[20] the fields must decay exponentially with y in the air region (y > d). Therefore, the transverse wave number can be defined by

$$\beta_2 = (\alpha^2 - P_2^2)^{1/2} \quad . \tag{2-11}$$

If radiation from the line is neglected, then β_2 will always be a real positive number as long as $k^2 > \omega^2 \mu_o \epsilon_o$, which is true for a slow wave. Radiation from the microstrip[25] becomes significant only when the line is in the form of an open-circuited resonator or a disc cavity resonator and has a large normalized substrate thickness ($d/\lambda_o > 0.01$) and/or a substrate of low dielectric constant ($K < 9$). The fields for the hybrid TM-TE mode are obtained by means of the following equations:[21]

$$\overline{E} = -j\omega\mu\nabla \times \overline{\pi}_h + \nabla \times \nabla \times \overline{\pi}_e$$

$$\overline{H} = \nabla \times \nabla \times \overline{\pi}_h + j\omega\epsilon\nabla \times \overline{\pi}_e \quad . \tag{2-12}$$

Using the boundary conditions that the tangential electric field and the normal derivative of the tangential magnetic field must be zero on the conductors and that the tangential magnetic field must vanish in the plane of symmetry x = 0, the following form of the potential functions for the lowest order hybrid mode may be written

$$\psi_e(\alpha, y) = A_s \cos\alpha x \sin\beta_1 y \qquad y < d$$

$$= B_s \cos\alpha x \exp[-\beta_2(y-d)] \qquad y > d$$

and

$$\psi_h(\alpha, y) = C_s \sin\alpha x \cos\beta_1 y \qquad y < d$$

$$= D_s \sin\alpha x \exp[-\beta_2(y-d)] \qquad y > d \tag{2-13}$$

where

$$\beta_1 = (P_1^2 - \alpha^2)^{1/2} \quad . \tag{2-14}$$

The coefficients A_s, B_s, C_s, and D_s, and thus all the field expressions, can be determined from the following boundary conditions at the interface between the substrate (region 1) and the air (region 2):

$$\mathcal{E}_{z1} = \mathcal{E}_{z2} \tag{2-15}$$

$$\mathcal{E}_{x1} = \mathcal{E}_{x2} \tag{2-16}$$

$$\mathcal{H}_{z1} - \mathcal{H}_{z2} = -I_x(\alpha) \tag{2-17}$$

$$\mathcal{H}_{x1} - \mathcal{H}_{x2} = I_z(\alpha) \quad . \tag{2-18}$$

All the above field quantities are Fourier transforms with respect to x of the real fields. The boundary conditions lead to a matrix, Eq. (2-19) shown below, from which the potential's coefficients can be obtained in terms of the two components of current on the strip and the unknown propagation constant k (see Appendix B):

$$\begin{bmatrix} a_{11} & a_{12} & 0 & 0 \\ 0 & 0 & a_{23} & a_{24} \\ a_{31} & a_{32} & a_{33} & a_{34} \\ a_{41} & a_{42} & a_{43} & a_{44} \end{bmatrix} \begin{bmatrix} A_s \\ B_s \\ C_s \\ D_s \end{bmatrix} = \begin{bmatrix} 0 \\ -jkI_x(\alpha)/P_2^2 \\ 0 \\ I_z(\alpha) \end{bmatrix} \tag{2-19}$$

where

$$a_{11} = \left(\frac{P_1}{P_2}\right)^2 \sin\beta_1 d \qquad a_{12} = a_{24} = -1$$

$$a_{23} = \left(\frac{P_1}{P_2}\right)^2 \cos\beta_1 d \qquad a_{31} = \alpha \sin\beta_1 d$$

$$a_{32} = -a_{44} = -\alpha \qquad a_{33} = \frac{\omega\mu_r\mu_o\beta_1}{k} \sin\beta_1 d$$

$$a_{34} = -\frac{\omega\mu_o\beta_2}{k} \qquad a_{41} = \frac{\omega K\epsilon_o\beta_1}{k} \cos\beta_1 d$$

$$a_{42} = \frac{\omega\epsilon_o\beta_2}{k} \qquad a_{43} = -\alpha \cos\beta_1 d$$

2. Analysis for Only Longitudinal Component of Current

As shown in Appendix A, the amplitude of the transverse component of current is proportional to the frequency and the strip width. Since most practical strip widths are very small compared to a wavelength (on the order of $0.01\lambda_o$), the transverse current is several orders of magnitude smaller than the longitudinal current. Thus, a good approximation to the exact microstrip solution would be to follow the same procedure as discussed in the previous section but make I_x equal to zero. The Hertzian potential coefficients A_s, B_s, C_s, and D_s can be solved easily from the matrix Eq. (2-19) and will be a function of the longitudinal component of current I_z and the unknown propagation constant (see Appendix B).

C. Derivation of Integral Equation for Phase Velocity

This section contains derivations of the integral equations for obtaining the microstrip phase velocity. The same two cases treated in Sec. II-B involving the current components are considered here.

1. Solution for Both Longitudinal and Transverse Currents

In anticipation of a slow-wave type of solution for a lossless microstrip line, the axial propagation constant (jk) is taken to be a pure imaginary quantity and the value of k is expected to be in the range $k_o \leqslant k \leqslant k_o\sqrt{\mu_r K}$, where $k_o = \omega\sqrt{\mu_o\epsilon_o}$. The quantity k along with the phase velocity v are of the form

$$k = \frac{2\pi}{\lambda_o}\sqrt{\xi}$$

and

$$v = v_o/\sqrt{\xi} \tag{2-20}$$

where

v_o = velocity of light in vacuo

λ_o = free-space wavelength

$$\xi = \mu_{eff}\epsilon_{eff}$$

μ_{eff} = effective relative permeability of microstrip line

and

ϵ_{eff} = effective relative dielectric constant of microstrip line .

ξ is found by using the following boundary conditions which result from the strip region being a perfect conductor:

$$E_{z2}(x, d) = 0 \qquad -w/2 < x < w/2 \quad . \tag{2-21}$$

$$\frac{dH_{z2}(x, d)}{dy} = 0 \qquad -w/2 < x < w/2 \quad . \tag{2-22}$$

Now, the total fields E_{z2} and H_{z2} are given by the following Fourier integral representation in terms of the coefficients B_s and D_s:

$$E_{z2}(x, y) = \int_{-\infty}^{\infty} \frac{P_2^2}{jk} B_s \cos \alpha x \exp[-\beta_2(y - d)]\, d\alpha \tag{2-23}$$

and

$$H_{z2}(x, y) = \int_{-\infty}^{\infty} \frac{P_2^2}{jk} D_s \sin \alpha x \exp[-\beta_2(y - d)]\, d\alpha \quad . \tag{2-24}$$

These expressions describe the longitudinal fields caused by the actual current distribution, which is nonzero only over the region occupied by the strip. Use of the relations for B_s and D_s given by Appendix B and the above boundary conditions results in the following coupled pair of integral equations involving the currents $I_z(\alpha) = I_{zo} J_o(\alpha w/2)$ and $I_x(\alpha) = I_{xo}[J_o(\alpha w/2)/\alpha w/2]$:

$$I_{xo} \int_{-\infty}^{\infty} \frac{j\left[\frac{\omega\mu_r\mu_o\beta_1 \tan\beta_1 d}{P_1^2} b_{22} + \frac{k\alpha}{P_1^2} b_{12}\right] \frac{J_o(\alpha w/2)}{\alpha w/2} \cos \alpha\eta}{Det(b_{ij})}\, d\alpha$$

$$- I_{zo} \int_{-\infty}^{\infty} \frac{b_{12} J_o(\alpha w/2) \cos \alpha\eta}{Det(b_{ij})}\, d\alpha = 0 \tag{2-25}$$

and

$$I_{xo} \int_{-\infty}^{\infty} \frac{j\beta_2\left[\frac{k\alpha}{P_1^2} b_{11} - \frac{\omega\mu_r\mu_o\beta_1 \tan\beta_1 d}{P_1^2} b_{21}\right] \frac{J_o(\alpha w/2)}{\alpha w/2} \sin \alpha\eta}{Det(b_{ij})}\, d\alpha$$

$$- I_{zo} \int_{-\infty}^{\infty} \frac{\beta_2 b_{11} J_o(\alpha w/2) \sin \alpha\eta}{Det(b_{ij})}\, d\alpha = 0 \tag{2-26}$$

where η is the value of x over the strip region $-w/2 \leqslant x \leqslant w/2$. The phase constant k, or the quantity ξ, can be found by setting the determinant of the coefficients of the unknown current amplitudes I_{xo} and I_{zo} to zero. It is quite apparent at this point that the computation time for such a solution will be enormous. A more practical solution is presented below.

2. Solution for Only Longitudinal Current

As mentioned previously, the strip width is very small compared to a wavelength, so that for the lowest order hybrid mode it suffices to satisfy Eqs. (2-21) and (2-22) only at the center of the strip $\eta = 0$ instead of over the range $-w/2 \leqslant \eta \leqslant w/2$. Thus, a single integral equation containing the unknown quantity ξ can be obtained from Eqs. (2-25) and (2-26) by setting both I_{xo} and η equal to zero. Substituting in the expressions for b_{ij} given in Appendix B, making a change of variable $\gamma = \alpha w$, and using Eq. (2-20), the integral equation becomes

$$\int_o^\infty \frac{\beta_1 Z I_z(\gamma)}{(YH)^2 + \frac{KZ}{\xi}\lambda_o^2 \beta_1 \left(Q \operatorname{ctn} \beta_1 d - \frac{\beta_2}{K\beta_1}\right)} d\gamma = 0 \qquad (2\text{-}27)$$

where

$$Y = \frac{\mu_r K - 1}{\mu_r K - \xi} \qquad Q = \frac{\xi - 1}{\mu_r K - \xi}$$

$$H = \frac{\lambda_o}{w}\gamma \qquad z = Q\mu_r \tan \beta_1 d + \frac{\beta_2}{\beta_1} \quad .$$

$$I_z(\gamma) = J_o\left(\frac{\gamma}{2}\right)$$

Note that the lower integration limit can be made zero since the integrand is an even function of γ. Also note that the amplitude I_{zo} of the current distribution function is not needed for the solution of ξ; only the part of the Fourier transform that is a function of γ is utilized.

As discussed in Sec. V, the alternate expression for the current Fourier transform given by Eq. (2-4) gives better than 1 percent accuracy for ξ and, furthermore, requires much less computer time. It is, in fact, the best function to use for microstrip lines having a large w/d ratio. This stems from the fact that the Maxwell current distribution is strictly correct for an isolated conducting strip, i.e., for the case where the ground plane is an infinite distance away from the strip. As the ground plane is brought closer, the ratio w/d increases and the current distribution approaches a more constant distribution across the strip width.[26] Using the change of variable in Eq. (2-4) results in the following alternate expression for $I_z(\gamma)$:

$$I_z(\gamma) = \frac{1}{\gamma}\left\{\frac{24}{\gamma^3} + \frac{3}{\gamma}\left(1 - \frac{\beta}{\gamma^2}\right)\cos\frac{\gamma}{2} + \left(1 - \frac{12}{\gamma^2}\right)\sin\frac{\gamma}{2}\right\} \quad . \qquad (2\text{-}28)$$

3. Determination of Characteristic Impedance

A definition for the characteristic impedance Z_o of the microstrip transmission line is in terms of the power P flowing along the longitudinal direction as well as the total current I flowing on the strip:

$$Z_o = P/I^2 \quad . \qquad (2\text{-}29)$$

An expression for power is obtained by integrating the z component of the Poynting vector $\overline{S} = \overline{E} \times \overline{H}^*$ over the cross section a' of the microstrip configuration as shown below:[21]

$$P = \frac{1}{2}\iint_{a'} (E \times H^*) \cdot \bar{a}_z \, dxdy \quad . \qquad (2\text{-}30)$$

The total current is obtained simply by integrating the current distribution $I_z(x)$ across the width of the strip

$$I = \int_{-w/2}^{w/2} I_z(x)\, dx \quad . \tag{2-31}$$

Thus, the expression for Z_o becomes

$$Z_o = \frac{\frac{1}{2}\int_{-\infty}^{\infty}\int_{o}^{\infty}\int_{-\infty}^{\infty}(\mathcal{E}_x \mathcal{H}_y^* - \mathcal{E}_y \mathcal{H}_x^*)\, dxdyd\alpha}{\left[\int_{-w/2}^{w/2} I_z(x)\, dx\right]^2} \quad . \tag{2-32}$$

The fact that the microstrip line is an open structure makes the computation of the above expression very lengthy. Therefore, from a practical standpoint, it is more reasonable to use a quasi-static definition in terms of the voltage V between the strip and the ground plane and the current I. Assuming that the width of the strip is small compared to a wavelength, the voltage can be obtained by taking the line integral of the vertical electric field component at the center of the strip. This integration is indeed not independent of the path for a propagating structure such as this, which has longitudinal field components. However, since the amplitudes of the latter are quite small, it is believed that the following expression for Z_o is a good approximation:

$$Z_o = \frac{V}{I} = \frac{\int_{o}^{\infty}\int_{o}^{d} \mathcal{E}_y dyd\alpha}{\int_{-w/2}^{w/2} I_z(x)\, dx} \quad . \tag{2-33}$$

Substituting the expression for $\mathcal{E}_y$ obtained from Eqs. (2-12) and (2-13) and that for $I_z(x)$ given by Eq. (2-3), the following integral represents the characteristic impedance in terms of the quantity ξ:

$$Z_o = \frac{192N\mu_r YQ}{w\sqrt{\xi}} \int_{o}^{\infty} \frac{\frac{H^2}{\beta_1} I_z(\gamma) \tan \beta_1 d}{(YH)^2 + \frac{KZ}{\xi}\lambda_o^2 \beta_1 \left(Q \operatorname{ctn} \beta_1 d - \frac{\beta_2}{K\beta_1}\right)} d\gamma \quad . \tag{2-34}$$

An even simpler expression for impedance can be obtained if one uses the following TEM definition, which should yield a good approximation since the microstrip's hybrid mode is very close to a TEM mode:

$$Z_o = \frac{1}{vC} = \frac{\mu_{eff}}{\sqrt{\xi}} Z_o \Big|_{K=1} \tag{2-35}$$

where

$C = \epsilon_{eff} C_o$ = capacitance/unit length

$C_o = C$ for $K = 1$, $\mu_r = 1$

$$v = \frac{v_o}{\sqrt{\xi}}$$

and

$$Z_o\Big|_{K=1} = \frac{1}{v_o C_o} = \text{characteristic impedance of air microstrip line} \quad .$$

The effective value of permeability μ_{eff} and the normalized propagation constant $\sqrt{\xi} = k/k_o$ are frequency-dependent quantities obtained from the integral equation (2-27) while $Z_o\Big|_{K=1}$ may be obtained from Wheeler's theory.[9]

4. Summary

The objective of this section has been to develop theoretical equations for the phase velocity and characteristic impedance of microstrip having a substrate made of either pure dielectric or demagnetized ferrite material. Numerical solutions of these equations for typical microstrip parameters are presented in Secs. V-A and V-B. The quantity $\xi = \mu_{eff}\epsilon_{eff}$ and the phase velocity are determined from Eqs. (2-27) and (2-20), respectively, if only the longitudinal current solution is used. Equations (2-25) and (2-26) must be used for the more exact solution involving both current components. The characteristic impedance is calculated by using Eq. (2-34) or (2-35).

III. THEORY FOR MAGNETIZED FERRITE-FILLED MICROSTRIP

A. Introduction

Propagation of electromagnetic waves along a microstrip line that is deposited on a ferrite substrate has been the subject of considerable interest for the past few years. It has been found especially fruitful to integrate a complete microstrip circuit that might include such gyromagnetic devices as meander-line phase shifters, isolators, and circulators, all deposited on a single ferrite substrate.[27] As long as operation is restricted well above the ferrite's natural resonant frequency f_m, defined in Sec. V-B, the microwave losses encountered when using a ferrite substrate are comparable with those obtained when pure dielectric substrates are utilized.

Even though a great amount of experimental work has been done involving ferrite-filled microstrip, it has not been matched by a corresponding theoretical investigation. A TE-TM mode solution for microstrip on a demagnetized ferrite substrate has been described in Sec. II, where the permeability was considered a scalar quantity which allows the fields to be expressed as a linear combination of TM and TE waves. The only other theoretical work on ferrite microstrip known by the author is that of Brodwin[6] who applied the parallel plane waveguide analysis of Van Trier[7] to a microstrip having a strip width on the order of half a wavelength. However, most practical microstrip lines have strip widths which are a small fraction of a wavelength (typically, $0.01\lambda_o$). It is very doubtful that Brodwin's theory for the latter case can be considered valid any longer. The purpose of this section is to present a theory that will describe the allowed propagating modes on a microstrip line whose width is a fraction of a wavelength and whose ferrite substrate is magnetized along the direction of propagation.

The microstrip configuration is the same as that shown in Fig. 1. Assuming the ferrite substrate to be a lossless medium, the relative dielectric constant K is, of course, a scalar quantity, while the relative permeability μ_r is a tensor whose components depend upon the ferrite's magnetization and the frequency. Given the above parameters as well as the strip width and the substrate thickness, the results derived here enable one to obtain the microstrip's phase velocity as a function of frequency. Also, the characteristic impedance can be calculated using the same quasi-static definition as in Sec. II.

B. Theory

As mentioned previously, the microstrip configuration has a cross section which is inhomogeneous, and the structure is an open waveguide with its natural propagating modes being surface waves if the source of the electromagnetic fields is located at infinity. Thus, transverse wave numbers must be purely real in the air region that extends to infinity. From the boundary conditions involving the continuity of fields at the substrate-air interface, it can be shown that no pure TEM, TE, or TM modes may exist. When the ferrite is demagnetized or when the fields in a magnetized medium exhibit perfect circular polarization, the permeability can be taken as a scalar quantity and the fields expressed as a summation of TM- and TE-mode fields. However, for the single microstrip line around which the fields cannot be considered circularly polarized and whose ferrite substrate is magnetized along the direction of propagation, the permeability is a tensor of the form

$$\overleftrightarrow{\mu}_r = \begin{bmatrix} \mu_1 & j\mu_2 & 0 \\ -j\mu_2 & \mu_1 & 0 \\ 0 & 0 & \mu_z \end{bmatrix} . \tag{3-1}$$

Substituting this tensor into Maxwell's equations yields two coupled wave equations involving the longitudinal field components

$$\left(\nabla_t^2 + \frac{\partial^2}{\partial z^2} + k_o^2 K\mu_\perp\right) E_z + k_o\mu_z \frac{\mu_2}{\mu_1} \frac{\partial}{\partial z} H_z = 0$$

and

$$\left(\nabla_t^2 + \frac{\mu_z}{\mu_1} \frac{\partial^2}{\partial z^2} + k_o^2\mu_z K\right) H_z - k_o K \frac{\mu_2}{\mu_1} \frac{\partial}{\partial z} E_z = 0 \tag{3-2}$$

where

$$\mu_\perp = \mu_1 - \frac{\mu_2^2}{\mu_1}$$

$$k_o = \omega \sqrt{\mu_o \epsilon_o}$$

and

ω = angular frequency .

Assuming propagation described by $e^{j(\omega t - kz)}$, where k is the phase constant along the axis of the DC magnetization, the above coupled equations can be converted to a fourth-order wave equation that contains a scalar potential ψ_F from which all the field quantities can be derived:[28]

$$(\nabla_t^2 + \chi_{1F}^2)\ (\nabla_t^2 + \chi_{2F}^2)\ \psi_F(x, y) = 0 \quad . \tag{3-3}$$

∇_t^2 is the transverse Laplacian operator and χ_{1F} and χ_{2F} are given by

$$\chi_{1F}^2,\ \chi_{2F}^2 = \frac{1}{2}\left[a + b \pm \sqrt{(a-b)^2 + 4c}\right] \tag{3-4}$$

where

$$a = k_o^2 K\left(\mu_1 - \frac{\mu_2^2}{\mu_1}\right) - k^2$$

$$b = \mu_z\left(k_o^2 K - \frac{\mu_2^2}{\mu_1}\right)$$

and

$$c = k^2 k_o^2 K \mu_z\left(\frac{\mu_2^2}{\mu_1}\right) \quad .$$

In this analysis, the axial propagation constant is assumed to be a pure imaginary quantity so that k is purely real and is of the form

$$k = k_o\sqrt{\xi} = \frac{\omega}{v} \quad . \tag{3-5}$$

For the microstrip configuration, it is convenient to choose the Cartesian coordinate system oriented as shown in Fig. 1 and to commence by taking a Fourier transform in the direction of the x-axis. The general representation for the scalar potential functions both in the air and the ferrite regions is

$$\psi(x, y) = \frac{1}{2\pi}\int_{C'} \psi(\alpha, y)\, e^{j\alpha x} d\alpha \quad . \tag{3-6}$$

In the air, the TE and TM mode scalar potential functions satisfy the wave equation

$$(\nabla_t^2 + P_2^2)\begin{Bmatrix}\psi_h(x, y)\\ \psi_e(x, y)\end{Bmatrix} = 0 \tag{3-7}$$

where $P_2^2 = k_o^2 - k^2$. Taking the Fourier transform with respect to x gives

$$\left(\frac{d^2}{dy^2} + k_o^2 - k^2 - \alpha^2\right)\begin{Bmatrix}\psi_h(\alpha, y)\\ \psi_e(\alpha, y)\end{Bmatrix} = 0 \quad . \tag{3-8}$$

[For the remainder of this analysis, ψ_e and ψ_h are understood to be Fourier transforms of the real potential functions given in Eq. (3-7)]. The transverse wave number is defined by

$$\beta_2 = (k^2 - k_o^2 + \alpha^2)^{1/2} \quad . \tag{3-9}$$

If radiating modes are neglected, the fields must decay exponentially with y in the air region. Therefore, β_2 will be a real positive number as long as $k^2 > \omega^2\mu_o\epsilon_o$, which is true for a slow wave. The contour C' that is used for computing the inverse Fourier transform in Eq. (3-6) can be chosen to be along the real axis since β_2 will be real for all values of α between $-\infty$ and ∞.

In the following, each Fourier component of the field will be forced to satisfy the boundary conditions of a grounded ferrite slab without the narrow conducting strip but having a fictitious surface current whose amplitude varies sinusoidally in the x direction along the substrate-air interface. The total fields are represented by a Fourier integral of the above components and must satisfy the continuity conditions at the interface as well as the boundary conditions at the strip, which is assumed to have the same surface current distributions as given in Sec. II-B-1. The effect of the conducting strip is to couple the TE and TM modes in the air and the modes existing in the ferrite substrate to create hybrid modes in which all field components are present. The coupling is interpreted as the requirement that the tangential electric field vanish on the strip. If the strip is assumed very narrow compared with a wavelength, this requirement is necessary only at the center of the strip.

Above the substrate's surface, the fields which are created by a single Fourier component of the surface current distribution can be simply expressed as a linear combination of TE- and TM-mode fields. They can be derived from the following set of Hertzian potential functions[24] for the lowest order hybrid mode:

$$\bar{\pi}_e = \bar{a}_z N \psi_e(\alpha, y)\, e^{j(\omega t - kz)}$$

and

$$\bar{\pi}_h = \bar{a}_z N \psi_h(\alpha, y)\, e^{j(\omega t - kz)} \tag{3-10}$$

where

$$\psi_e = G_t\, e^{-\beta_2(y-d)} \cos \alpha x$$

and

$$\psi_h = F_t\, e^{-\beta_2(y-d)} \sin \alpha x \quad . \tag{3-11}$$

Leaving out the z and t dependence of $N\, e^{j(\omega t - kz)}$, where N is an arbitrary constant, the fields are given in terms of the above scalar potentials as follows:[24]

$$\mathcal{E}_{z2} = \frac{P_2^2}{jk}\, \psi_e$$

$$\mathcal{H}_{z2} = \frac{P_2^2}{jk}\, \psi_h$$

$$\bar{\mathcal{E}}_{T2} = -\nabla_T \psi_e - \frac{\omega \mu_o}{k} (\nabla_T \psi_h \times \bar{a}_z)$$

and

$$\bar{\mathcal{H}}_{T2} = -\nabla_T \psi_h - \frac{\omega \epsilon_o}{k} (\bar{a}_z \times \nabla_T \psi_e) \quad . \tag{3-12}$$

In the ferrite region, the potential function that satisfies the fourth-order wave Eq. (3-3) is expressed as a linear combination of solutions corresponding to the two possible eigenvalues in the following manner:

$$\psi_F(\alpha, y) = \psi_{1F} + \psi_{2F} \tag{3-13}$$

where

$$\psi_{1F} = (A_t \sin\beta_{1F} y + C_t \cos\beta_{1F} y)\, e^{j\alpha x}$$

and

$$\psi_{2F} = (B_t \sin\beta_{2F} y + D_t \cos\beta_{2F} y)\, e^{j\alpha x} \quad .$$

The sine and cosine dependence is chosen in order to satisfy the boundary conditions on the conductor and to include both the symmetric and antisymmetric modes. The transverse wave numbers β_{1F} and β_{2F} are given in terms of the eigenvalues χ_{1F} and χ_{2F}, respectively, by the relations:

$$\beta_{1F}^2 = \chi_{1F}^2 - \alpha^2$$

and

$$\beta_{2F}^2 = \chi_{2F}^2 - \alpha^2 \quad . \tag{3-14}$$

Note that values of α and k are common to both the air and the ferrite region since these quantities are given by the exciting current. In terms of $\psi_F(\alpha, y)$, the Fourier components of the fields can now be written as[28]

$$\bar{\mathcal{E}}_1 = \begin{bmatrix} jS_F & T_F & 0 \\ -T_F & jS_F & 0 \\ 0 & 0 & jW_F \end{bmatrix} \nabla\psi_F(\alpha, y) \tag{3-15}$$

and

$$\bar{\mathcal{H}}_1 = -jk \begin{bmatrix} jM_F & N_F & 0 \\ -N_F & jM_F & 0 \\ 0 & 0 & jR_F \end{bmatrix} \nabla\psi_F(\alpha, y) \tag{3-16}$$

with

$$S_F = \frac{\mu_2}{\mu_1} k^2$$

$$T_{1F,\,2F} = k_o^2 K \left(\frac{\mu_1^2 - \mu_2^2}{\mu_1} \right) - k^2 - \chi_{1F,\,2F}^2$$

$$W_{1F,\,2F} = -\frac{\mu_2}{\mu_1} \chi_{1F,\,2F}^2$$

$$M_{1F,\,2F} = \frac{1}{\mu_1 k_o}\left(k_o^2 K\mu_1 - k^2 - \chi_{1F,\,2F}^2\right)$$

$$N_F = k_o K \frac{\mu_2}{\mu_1}$$

and

$$R_{1F,\,2F} = -\frac{T_{1F,\,2F}\chi_{1F,\,2F}^2}{k_o \mu_z k^2} \quad .$$

In the above relationships, the subscripts 1F and 2F are associated with the potential functions ψ_{1F} and ψ_{2F}, respectively. The following boundary conditions must be used to solve for the six unknown coefficients, A_t, B_t, C_t, D_t, G_t, and F_t:

$$\mathcal{E}_{z1} = 0 \quad \text{at} \quad y = 0 \tag{3-17}$$

and

$$\frac{\partial \mathcal{H}_{z1}}{\partial y} = 0 \quad \text{at} \quad y = 0 \tag{3-18}$$

and at the substrate-air interface y = d,

$$\mathcal{E}_{z1} = \mathcal{E}_{z2} \tag{3-19}$$

$$\mathcal{H}_{z1} - \mathcal{H}_{z2} = -I_x(\alpha) \tag{3-20}$$

$$\mathcal{E}_{x1} = \mathcal{E}_{x2} \tag{3-21}$$

and

$$\mathcal{H}_{x1} - \mathcal{H}_{x2} = I_z(\alpha) \quad . \tag{3-22}$$

Boundary conditions (3-17) and (3-18) can be used to express A_t and C_t in terms of the other coefficients; the remaining boundary conditions (3-19) through (3-22) lead to the following set of simultaneous equations:

$$a_{11}B_t + a_{12}D_t + a_{13}G_t + 0 = 0$$

$$a_{21}B_t + a_{22}D_t + 0 + a_{24}F_t = -I_x(\alpha)$$

$$a_{31}B_t + a_{32}D_t + a_{33}G_t + a_{34}F_t = 0$$

and

$$a_{41}B_t + a_{42}D_t + a_{43}G_t + a_{44}F_t = I_z(\alpha) \quad . \tag{3-23}$$

The coefficients a_{ij} are given in Appendix C along with the six potential coefficients.

In order to obtain the propagation constant, use is made of the boundary conditions that E_{z2} and $\partial H_{z2}/\partial y$ must vanish on the conducting strip. This results in a pair of integral equations which involve the two components of current. They are similar to Eqs. (2-25) and (2-26). If the strip width is assumed to be small compared to a wavelength and the transverse current I_x is neglected, then the equation for the propagation constant reduces to

$$\int_{-\infty}^{\infty} \frac{P_2^2}{jk} Z_1 I_z(\alpha)\, d\alpha = 0 \qquad (3\text{-}24)$$

where Z_1 is given in Appendix C. Since the integrand contains linear terms in μ_2/μ_1, the propagating modes must be of a nonreciprocal nature. Also, the tensor property of the magnetized ferrite substrate allows a number of symmetric and antisymmetric modes to propagate. The types of modes are expected to be similar to that obtained for a ferrite-loaded wire[29] and a ferrite-filled coaxial transmission line.[30]

C. Summary

In this section equations were derived for the propagation constants and the electromagnetic fields of magnetized ferrite-filled microstrip. The former can be obtained by the use of Eq. (3-24), while the field expressions require the combination of Eqs. (3-11) through (3-16). Because the dependence of permeability on saturation magnetization, applied field, and frequency is not known for the ferrite slab configuration, the scope of this study does not include any calculations for the magnetized microstrip case. Once the permeability expressions are known, then the contents of this section may be utilized to predict the various propagating modes.

IV. THEORY FOR A COUPLED PAIR OF MICROSTRIP LINES

A. Introduction

Coupled microstrip lines, which are deposited onto the surface of the substrate, as shown in Fig. 4, can be used in microstrip integrated circuits for making directional couplers, bandpass filters, band reject filters, and reaction cavities. They are also the basic elements in such slow-wave structures as meander lines and interdigital lines. The latter planar devices are capable of producing nonreciprocal differential phase shift, which is of great utility in phased array radar. However, the relation between the nonreciprocal properties of these devices and the geometry of the microstrip lines has not yet been thoroughly investigated.

The static solution for two coupled lines on a pure dielectric substrate has been obtained by Bryant and Weiss.[16] Their results show that this microstrip configuration supports both even and odd modes which have different phase velocities. As can be expected, the even- and odd-mode characteristic impedances are also quite different. This section presents a TE-TM mode

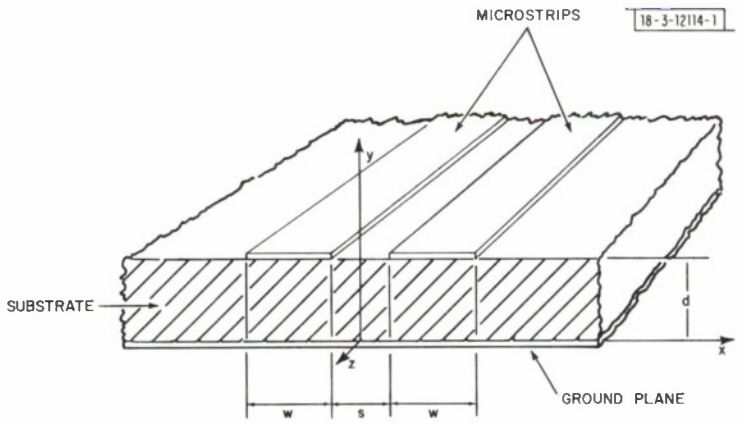

Fig. 4. Coupled pair of microstrip lines.

solution that will give the frequency dependence of the even- and odd-mode velocities and characteristic impedances for a coupled pair of microstrip lines. Four different cases will be treated: (1) a pure dielectric substrate having no nonreciprocal effects, (2) a demagnetized ferrite substrate having a scalar permeability as well as a scalar permittivity, (3) a magnetized ferrite substrate whose permeability can be considered scalar when the lines are in a configuration that produces circular polarization between them, as is the case for a meander line, and (4) a magnetized ferrite substrate whose permeability is a tensor with off-diagonal terms. For the last two cases, it is assumed that the applied magnetic field is along the direction of propagation. In addition, the analysis for each case contains assumptions that the structure is lossless and that the fields vary as $e^{j(\omega t - kz)}$, where the phase constant k is pure real.

The theory is then applied to two commonly used microstrip devices, namely, the quarter-wave directional coupler and the meander-line phase shifter.

B. Determination of the Even- and Odd-Mode Fields and Propagation Constants

The theory for propagation on a coupled pair of microstrip lines, or for any number of parallel, coplanar microstrip lines, is a simple extension of that presented in Secs. II and III. First, a solution is obtained for the sinusoidal surface current distribution at the substrate-air interface. Then, a Fourier integral of these "fictitious" sinusoidal components is formed in order to represent the fields caused by the actual current distribution, which now is nonzero over two strip regions of equal dimensions that are symmetric about the origin, as shown in Fig. 4. For the even mode of propagation, the direction of the current is the same for both strips and, therefore, exhibits even symmetry with respect to reflection in a central bisecting plane. On the other hand, the odd mode with equal currents flowing in opposite directions has odd symmetry with respect to that same plane.

The Green's function method of Bryant and Weiss is again used to estimate the current distribution on the pair of coupled lines. Since the spatial distribution of charge is dependent on the parameters w/d and s/d, where s is the spacing between adjacent edges of the strip, it is now much more difficult to arrive at an analytical expression for $I_z(x)$ that will give reasonably accurate results. Thus, in order to get $I_z(\alpha)$, a discrete Fourier transform of the charge data obtained from the Green's function method is formed.

In Bryant and Weiss's numerical solution, the strips and the space between them are divided into elements of width $\Delta x/d$, which is chosen equal to 0.025 in order to provide sufficient accuracy in treating most practical microstrip lines. Their Green's function solution ϕ_{ij} gives the potential at the i^{th} element due to the j^{th} element carrying unit charge. The values of charge q_i on the i^{th} element of the m elements comprising the normalized strip width, $w/d = m(\Delta x/d)$, are then found by solving a set of m simultaneous equations:

$$\sum_{j=1}^{m} q_j(\phi_{ij} \pm \phi_{i,\, 2m+N_s+1-j}) = V \qquad (4\text{-}1)$$

where

V = potential of the strip .

This gives the desired current distribution for the microstrip propagation problem as

$$I_{zoi} = I_{oo} q_{oi} \qquad \text{(odd mode)}$$

and

$$I_{zei} = I_{oe} q_{ei} \qquad \text{(even mode)} \tag{4-2}$$

where I_{oo} and I_{oe} are proportionality constants. The total currents I_{zod} and I_{zev} flowing on the strip are simply a summation of the above equations over values of i between 1 and m. Taking the discrete Fourier transform of this current distribution yields

$$I_{zo}(\gamma) = I_{oo} \sum_{p=N_s}^{N_s+m} q_p \sin\left(\frac{\gamma}{w/d} \frac{\Delta x}{d}\right) p \qquad \text{(odd mode)}$$

and

$$I_{ze}(\gamma) = I_{oe} \sum_{p=N_s}^{N_s+m} q_p \cos\left(\frac{\gamma}{w/d} \frac{\Delta x}{d}\right) p \qquad \text{(even mode)} \tag{4-3}$$

where

$$\gamma = \alpha w$$

$$\frac{\Delta x}{d} = 0.025 \quad .$$

The integral equation for obtaining the even- and odd-mode propagation constants will then contain the above series expressions for the current transform $I_z(\gamma)$ instead of the analytic expressions used in Secs. II and III.

Referring to the four possible cases of microstrip propagation listed in Sec. IV-A, the first three involve both a scalar permeability and a scalar permittivity. If only longitudinal currents are assumed to flow on the conductors, then these cases will require the use of integral Eq. (2-27) subject to the above change in the current transform. For the magnetized ferrite case in which the permeability is a tensor quantity, Eqs. (3-24) and (4-3) must be used to obtain the even- and odd-mode propagation constants. Due to symmetry and the fact that the conducting strips are now situated at $x = \pm(s + w/2)$ instead of at the origin, the integrands of these integral equations must be multiplied by $\cos\alpha(s + w/2)$ for the even mode and $\sin\alpha(s + w/2)$ for the odd mode.

C. Characteristic Impedance

The same kind of quasi-static definition involving voltage and current used for the single strip (see Sec. II-C-3) will be used here to obtain the characteristic impedance associated with the even and odd modes of propagation on the coupled microstrip structure. However, the paths of integration as well as the field components involved are different. The validity of these rather arbitrary definitions can be tested once a measurement technique that accounts for connector mismatch is established.

For the odd mode, symmetry dictates that the plane $x = 0$ be at ground potential and the two strips be at a potential of +V and −V, respectively. Thus, the odd-mode characteristic impedance Z_{oo} can be defined as the ratio of the voltage V_o between the strip and the bisecting plane

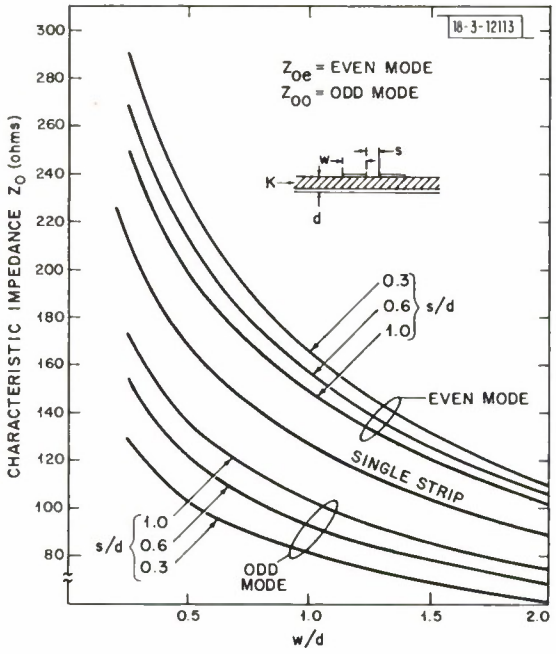

Fig.5. Characteristic impedance of caupled pair of microstrip lines for K = 1.

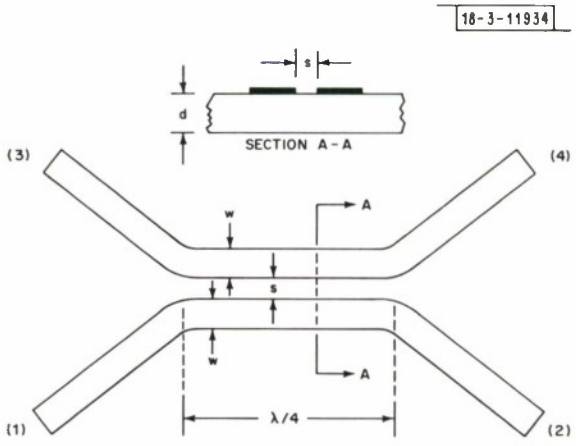

Fig.6. Microstrip directianal caupler.

to the total current flowing on a strip I_{zod}. Expressing V in terms of the line integral of the electric field gives

$$Z_{oo} = \frac{\int_{-\infty}^{\infty} \int_{o}^{s/2} \mathcal{E}_x \Big|_{y=d} \, dx d\alpha}{I_{zod}} \quad . \tag{4-4}$$

For the even mode, both strips are at a potential $+V_e$ with respect to the ground plane and each strip carries half the total current $2I_{zev}$. The even-mode characteristic impedance Z_{oe} per strip to ground is then given by the ratio of V_e to I_{zev}. In terms of the electric field and the current distribution function Z_{oe} becomes

$$Z_{oe} = \frac{\int_{-\infty}^{\infty} \int_{o}^{d} \mathcal{E}_y \Big|_{x=(s+w)/2} \, dy d\alpha}{I_{zev}} \tag{4-5}$$

where I_{zev} is given in Sec. IV-B. Note that the line integral of the vertical electric field component can be taken at the center of the strip if it is assumed that the strip width is small compared to a wavelength.

More approximate expressions for characteristic impedance can be obtained by using the TEM definitions

$$Z_{oo} = \frac{\mu_{eff\,od}}{\sqrt{\xi_o}} \, Z_{oo} \Big|_{K=1}$$

and

$$Z_{oe} = \frac{\mu_{eff\,ev}}{\sqrt{\xi_e}} \, Z_{oe} \Big|_{K=1} \tag{4-6}$$

The impedances for the air microstrip line (K = 1) are obtained from Bryant and Weiss's TEM solution. Their dependence on w/d and s/d is illustrated in Fig. 5. The above impedance equations agree very well with the more complex set of Eqs. (4-4) and (4-5) at zero frequency. However, the relative merit of these two sets of impedance equations for finite values of frequency has not been determined because of the lack of an adequate measurement technique.

D. Application to a Directional Coupler

The theory that has been presented on coupled microstrip lines is directly applicable to the design of the microstrip quarter-wave directional coupler, shown in Fig. 6. With pure TEM lines, such as the stripline configuration, one can design a broadband directional coupler for any degree of coupling. However, the asymmetry of microstrip with its imbalance of even- and odd-mode phase velocities results in a narrow bandwidth and what has been experimentally found to be a finite directivity limit for tight coupling.[31]

The scattering matrix for a microstrip directional coupler with lines of characteristic impedance Z_o connected to all four ports is a function of the even- and odd-mode velocities and impedances (v_{ev}, v_{od}, Z_{oe}, Z_{oo}, respectively) and has the form

$$[S_c] = \begin{bmatrix} A_c & B_c & C_c & D_c \\ B_c & A_c & D_c & C_c \\ C_c & D_c & A_c & B_c \\ D_c & C_c & B_c & A_c \end{bmatrix} . \qquad (4\text{-}7)$$

The quantities A_c, B_c, C_c, and D_c are given for convenience in Appendix D. In the special case where $v_{ev} = v_{od}$ and $Z_o = (Z_{oe}Z_{oo})^{1/2}$, the matrix terms A_c and D_c are both equal to zero, which makes the device a perfect coupler. This can only hold true for TEM transmission lines. However, for the microstrip case, all the terms are finite due to the unequal phase velocities which cause the coupler to exhibit poor directivity and narrow bandwidth.

To the best of our knowledge, no experimental results on ferrite-filled microstrip directional couplers have been reported to date in the literature. Since this report gives equations for calculating the even- and odd-mode velocities and impedances for both a dielectric and a ferrite substrate, there is more flexibility in choosing the geometry and substrate material for the microstrip device. In order to improve the coupler's performance, the phase velocities must be brought closer together. As illustrated by the theoretical and experimental results described in Sec. V-D, this can be accomplished in a microstrip with a demagnetized ferrite substrate if operation is restricted to a frequency band corresponding to values of normalized saturation magnetization m_s (defined in Sec. V-B) between about 0.4 and 1.0.

E. Application to a Meander-Line Phase Shifter

In order to get a nonreciprocal interaction with a ferrite substrate, a microwave circuit which produces circularly polarized magnetic fields in the ferrite material is required. A circuit component that can achieve this is a meander line that consists of a periodic array of the basic element shown in Fig. 7. By making the meander path length ℓ a quarter-wavelength, both time quadrature and space quadrature of the RF magnetic fields will be provided at point A. If a DC internal field is applied parallel to the strip, as shown in Fig. 7, the magnetic moments in the ferrite material will precess in a circular orbit about the steady internal field vector. If this precession is in coincidence with the signal circular polarization established by the meander-line circuit, there will be strong coupling and enhancement of phase delay for one direction of propagation, but very weak coupling and an opposition to phase delay for the opposite direction. This produces the desired "differential" phase shift, the amount of which depends upon the strength of the applied field, the ferrite material's saturation magnetization, and the frequency.

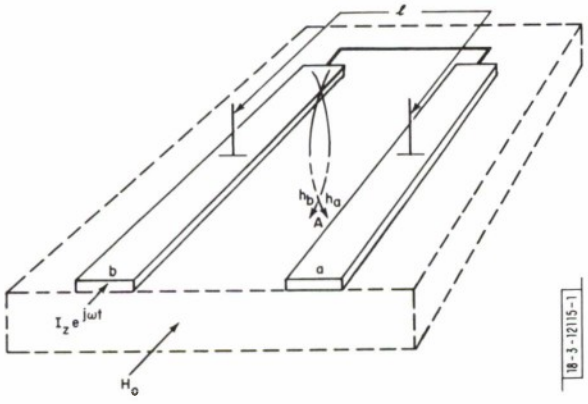

Fig. 7. Basic element of meander-line phase shifter.

The analysis of this ferrite device is quite complex because of the fact that the degree of RF magnetic field circular polarization not only varies from purely circular at the center of the lines through elliptical to linear at its ends, but also varies throughout the cross section of the line,

i.e., perpendicular to the direction of propagation. Another complication for meander lines having a small pitch (period of repetition of the basic elements) is the dispersion of the microwave circuit due to coupling between nonadjacent elements. Butcher[32] only studies this effect for a meander-line structure without the presence of a ground plane or any dielectric discontinuity. Thus, there exists at present no way of theoretically predicting the amount of differential phase for this device.

There has been some recent work in obtaining a design procedure for yielding a matched meander line. Hair and Roome[27] used an iterative-type procedure based on an infinite number of meanders and involving the reading of several sets of curves which give various fringing capacitances. Their analysis falsely assumes equal impedances and velocities for the even and odd modes that propagate on the meander line.

A recent Ph.D. dissertation by Libbey[33] contains a more valid approach for the case of a few meanders. The differences in the velocities and in the impedances are accounted for by a modification of Jones and Bolljahn's[34] all-pass filter equations. Libbey's derived expressions for image impedance Z_I and insertion phase ϕ_I of the single meander, shown in Fig. 7, are given below.

$$Z_I = \sqrt{Z_{oe} Z_{oo}} \sqrt{\frac{\tan k_{od}\ell}{\tan k_{ev}\ell}} \tag{4-8}$$

and

$$\cos \phi_I = \frac{(Z_{oe}/Z_{oo}) - \tan k_{ev}\ell \tan k_{od}\ell}{(Z_{oe}/Z_{oo}) + \tan k_{ev}\ell \tan k_{od}\ell} \tag{4-9}$$

where

$$k_{od} = \frac{\omega}{v_{od}}$$

and

$$k_{ev} = \frac{\omega}{v_{ev}} \quad .$$

The dynamic theory for coupled microstrip lines given in Secs. IV-C and IV-D can now be used for determining Z_I and ϕ_I. The only difficulty that remains is the question of what expression to use for the permeability of the magnetized ferrite substrate. If it is assumed that the fields are circularly polarized and that the effect of the short meander-line section oriented perpendicular to the applied field is neglected, then the permeability for the forward (+) and reverse (−) directions of propagation can be taken as scalar quantities

$$\mu^+ = \mu_1 - \mu_2 \tag{4-10}$$

and

$$\mu^- = \mu_1 + \mu_2 \tag{4-11}$$

where μ_1 and μ_2 are the diagonal and off-diagonal components of the permeability tensor, respectively. These components are known for the case of an infinite ferrite medium[35] but not for the microstrip slab configuration. Schlömann[36] recently obtained a solution for the effective

permeability tensor components of a magnetized ferrite configuration consisting of an arbitrary number of concentric, cylindrical, magnetic domains which are oriented along the cylinder's axis either parallel or anti-parallel to the applied DC magnetic field. This theory may be applicable to microstrip if one views the ferrite substrate as being composed of a large number of cylindrical magnetic domains oriented either parallel or anti-parallel to the direction of propagation and the applied field H_o. The forms taken by Schlömann's theoretical curves of permeability versus relative magnetization M/M_s for a ferrite sample having at least 80 domains were nearly parabolic in the case of the diagonal component $\mu_{1\,\mathrm{eff}}$ and approximately linear in the case of the off-diagonal component $\mu_{2\,\mathrm{eff}}$. As a result, the following equations were derived from these curves:

$$\mu_{1\,\mathrm{eff}} = \mu_{\mathrm{min}} + (1 - \mu_{\mathrm{min}})\,(M/M_s)^2 \tag{4-12}$$

and

$$\mu_{2\,\mathrm{eff}} = m_s(M/M_s) \tag{4-13}$$

where

$$\mu_{\mathrm{min}} = (1 - m_s^2)^{1/2}$$

$$m_s = 2.8(4\pi M_s)/f \quad , \quad \text{as defined in Sec. V-B} \quad .$$

Substituting these expressions into Eqs. (4-10) and (4-11) results in the following scalar permeabilities for the circularly polarized case:

$$\mu^+ = \mu_{\mathrm{min}} + (1 - \mu_{\mathrm{min}}) \left(\frac{M}{M_s}\right)^2 - m_s \left(\frac{M}{M_s}\right) \tag{4-14}$$

and

$$\mu^- = \mu_{\mathrm{min}} + (1 - \mu_{\mathrm{min}}) \left(\frac{M}{M_s}\right)^2 + m_s \left(\frac{M}{M_s}\right) \quad . \tag{4-15}$$

As illustrated in Sec. V-E, these equations can then be used in the propagation constant integral equations that are applicable for both a scalar permeability and a scalar permittivity.

F. Summary

This section has been devoted to the dynamic theory for a coupled pair of microstrip lines on both a dielectric and a ferrite substrate. For the cases in which the substrate can be characterized by a scalar permeability as well as a scalar permittivity, integral Eq. (2-27) is utilized in conjunction with a discrete Fourier transform of the static current distribution given by Eq. (4-3) to obtain the coupled microstrip's even- and odd-mode propagation constants. The numerical results for typical microstrip parameters are described in Secs. V-C, V-D and V-E. As soon as the permeability is known for the magnetized ferrite substrate, Eqs. (3-24) and (4-3) can be used to obtain the magnetized coupled microstrip propagation constants.

V. PRESENTATION AND DISCUSSION OF THEORETICAL AND EXPERIMENTAL RESULTS

The numerical solutions of the theoretical equations obtained in preceding sections are discussed below and, in some cases, compared with experimental results. Cases for a pure

dielectric substrate as well as a demagnetized or magnetized ferrite substrate will be covered. The microstrip geometry and material are chosen to represent typical microwave integrated circuit applications.

Using a digital computer to solve integral Eq. (2-27) for the quantity ξ, it was only necessary to sum over values of the integration variable γ between 0 and 100 in order to acquire accuracy to within the fourth decimal place, because the integrand converged quite rapidly. A half-interval search technique (subroutine TRANS) was used to find the roots of the equation. All the computer programs in Fortran IV language and the flow chart are given in Appendix E.

A. Single Microstrip Line on a Pure Dielectric Substrate

In order to establish the validity of the theory presented in Sec. II, it was necessary to initially make a comparison with the static solutions of Bryant and Weiss[16] by solving for $\xi = \epsilon_{eff}$ at zero frequency. Longitudinal current solutions were obtained using the Fourier transforms for both current distributions given by Eqs. (2-27) and (2-28) and the results plotted as a function of K and w/d, as shown in Figs. 8 and 9, respectively. The first curve, which was calculated for a w/d ratio of 0.4, showed that the use of the Maxwell distribution for the current produces results that agree almost exactly (within 0.2 percent) with Bryant and Weiss's solution, whereas the current distribution of Eq. (2-28) yields a solution which is about 0.6 to 0.8 percent low. With K held constant, Fig. 9 shows that the solution utilizing the Maxwell function agrees best with the recent static solutions mentioned in Sec. I for w/d values in the range $o < w/d \leqslant 1.2$, while the current distribution function of Eq. (2-28) yields better agreement for higher w/d values ($w/d > 1.2$). If the least amount of computer time is desired, then the use of the latter function, which is accurate to better than 1 percent for all values of w/d and K, is recommended.

The complete solution described by Eqs. (2-25) and (2-26) was found to require a large amount of computer time. A couple of points were computed and the results were in excellent agreement with the longitudinal current solution both at zero frequency and at a finite frequency. It was concluded that the solution which neglects the transverse current is a very good approximation.

In regard to the characteristic impedance Z_o, the zero frequency values calculated from Eq. (2-34) with N equal to unity agree within 1 percent of Wheeler's results,[9] which are the most accurate of the available TEM solutions for small w/d values (< 0.2). The theoretical equation for Z_o that involves a line integral in the plane $x = 0$ necessarily implies that a very narrow strip is considered. However, Fig. 10 illustrates that better than 1 percent accuracy can be obtained for wider strips by choosing a normalization constant N of 0.95. Figure 11 shows the variation of Z_o with substrate dielectric constant K.

Returning to Eq. (2-27) and solving for $\xi = \epsilon_{eff}$ as a function of frequency results in a dispersion curve, illustrated by Fig. 12. Note that the curve asymptotically approaches the substrate's dielectric constant at very high frequencies, indicating that all the energy is being confined to the dielectric. The phase velocity v can now be obtained from Eq. (2-20); its frequency dependence is shown in Fig. 13. An interesting observation is that this curve has an inflection point at which the velocity starts to approach the value $v_o/\sqrt{K}$ and is given by the following equation:

$$f_c = \frac{v_o}{4d\sqrt{K-1}} \quad . \tag{5-1}$$

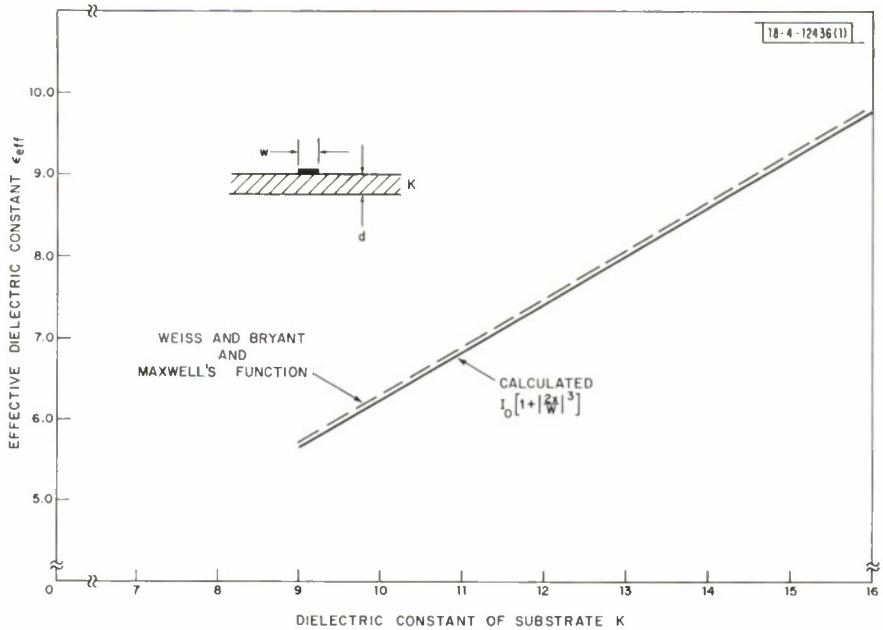

Fig. 8. Effective dielectric constant versus K: w/d = 0.40.

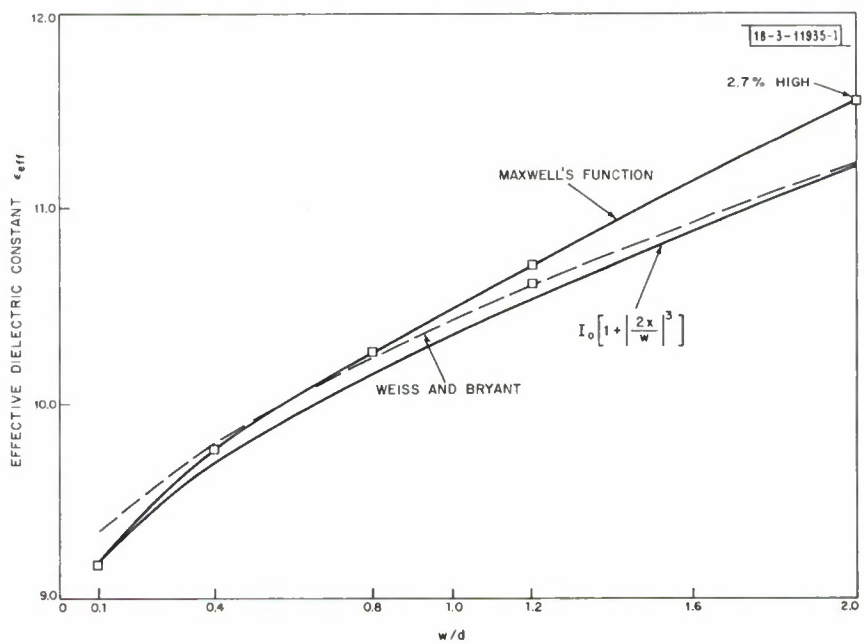

Fig. 9. Effective dielectric constant versus w/d: K = 16.

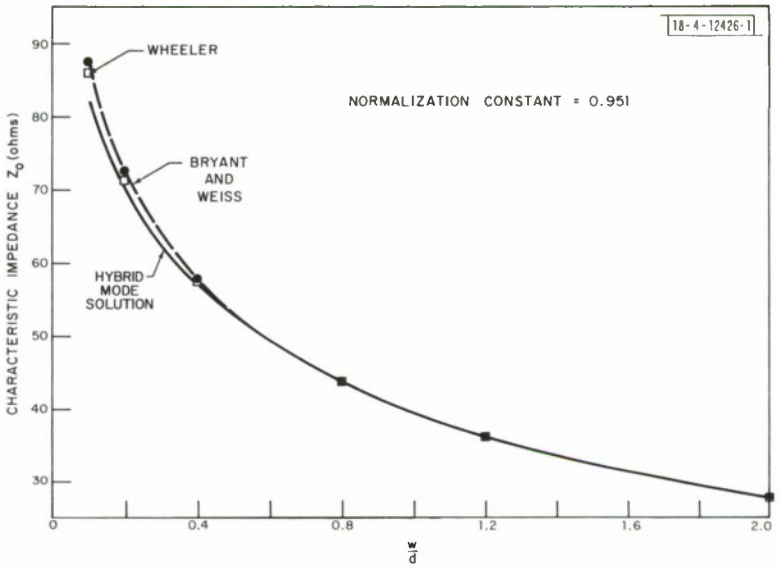

Fig. 10. Characteristic impedance versus w/d: K = 16.

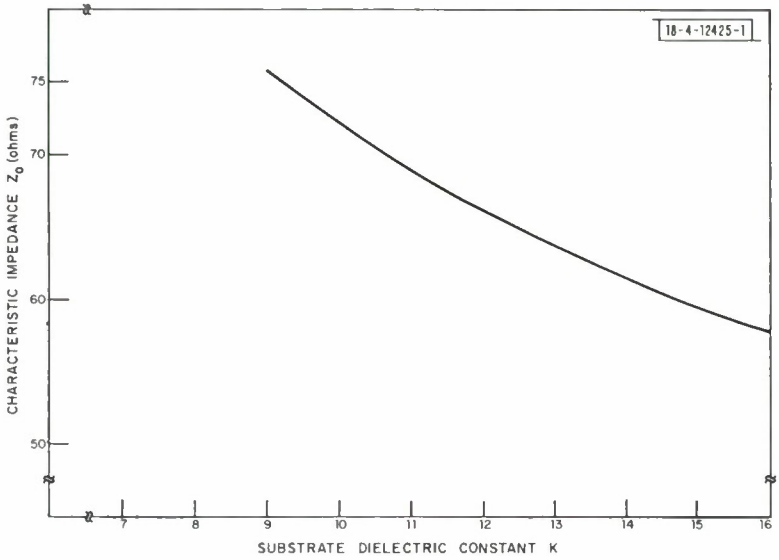

Fig. 11. Characteristic impedance versus K: w/d = 0.40.

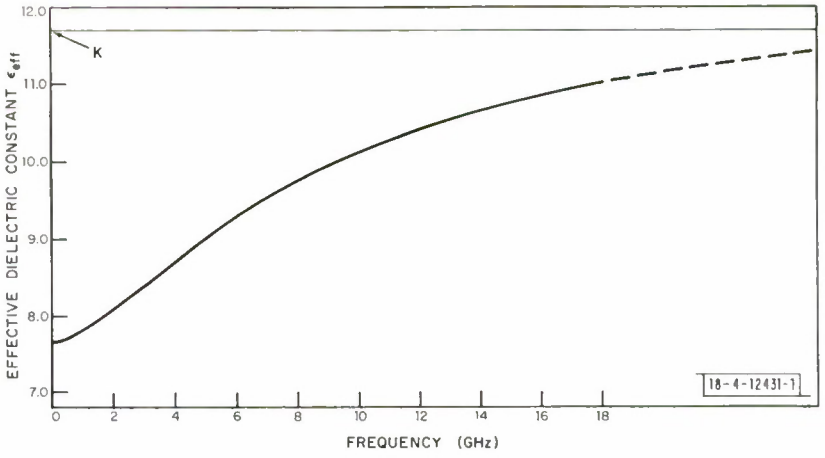

Fig. 12. Effective dielectric constant versus frequency: K = 11.7, w/d = 0.96, d = 0.317 cm, $d/\lambda_o\big|_{f=1\ GHz} = 0.0106$.

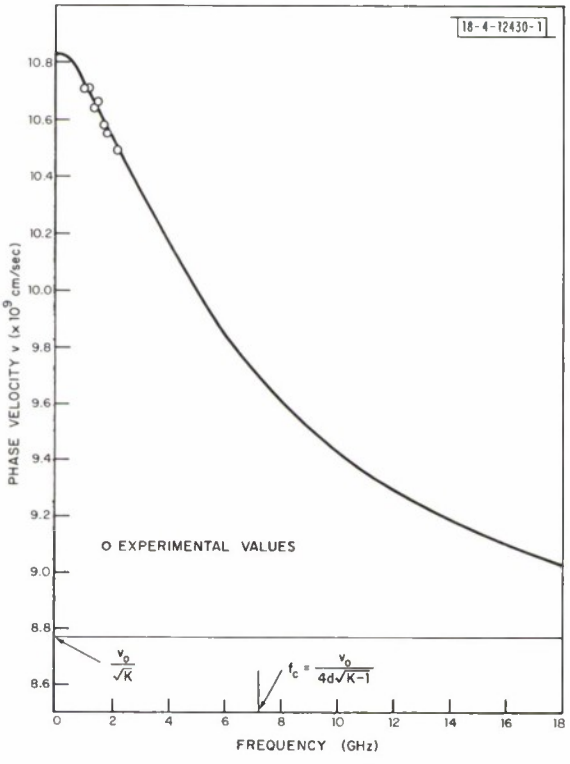

Fig. 13. Phase velocity versus frequency: K = 11.7, w/d = 0.96, d = 0.317 cm, $d/\lambda_o\big|_{f=1\ GHz} = 0.0106$.

This same frequency was defined by Hartwig, et al.,[15] as the "divergence frequency" above which the propagation of energy is not confined to the microstrip configuration, but is coupled to a TE_1 surface wave. Consequently, for frequency $f > f_c$, the energy can propagate along the surface of the substrate in all directions and will radiate from the edges.

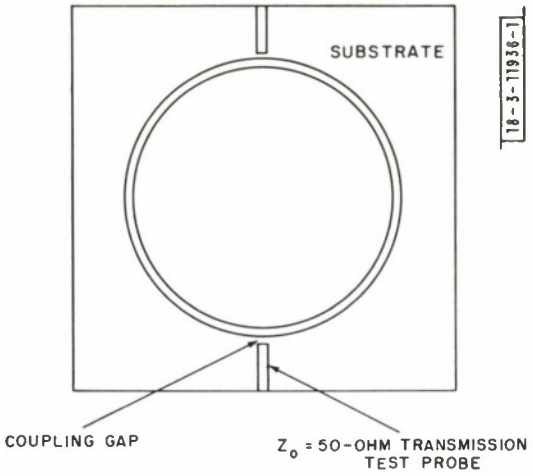

Fig. 14. Ring resonator.

An experimental check of the above frequency dependence of velocity can easily be accomplished by the use of a microstrip resonator which is in the form of a ring[37] or a straight open-ended line. The former, shown in Fig. 14, is employed whenever end effects associated with the straight-line resonator become significant. It is seldom useful for low-frequency measurements (typically, <3 GHz) since the length must be at least five wavelengths in order to avoid the effects of mutual inductance. However, the fringing effects of an open circuit are negligible at the low-frequency end, so that here the multiple half-wavelength long, straight-line resonator can be used.

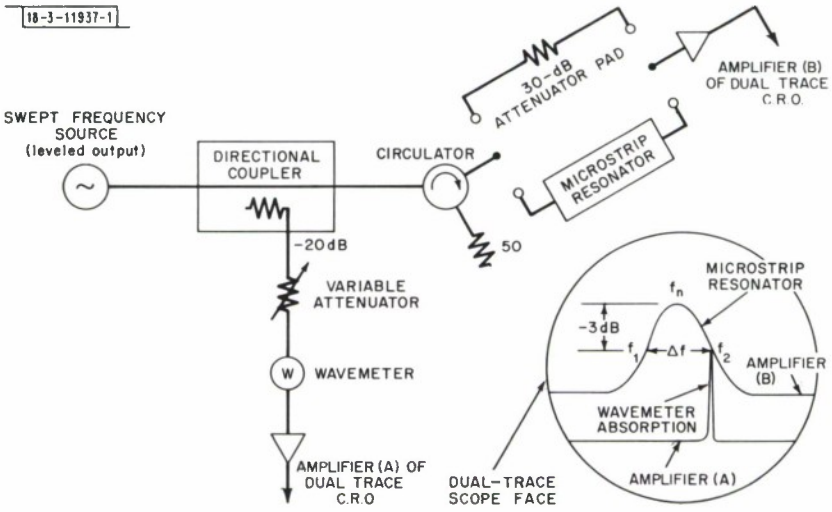

Fig. 15. Experimental arrangement for velocity measurement.

Figure 15 shows the experimental arrangement for measuring the microstrip line's phase velocity with the use of either one of the resonators mentioned above. Transmission Q-factor measurements are made using sweep gear, and the coupling gap to either the ring or to the end of a straight microstrip line is adjusted until the unloaded Q factor is measured. This occurs whenever there is no further increase in the value of Q with increasing gap size and is usually at a level of −30 dB relative to straight-through transmission without the resonator. Knowing the mean length of the ring or the straight line, the resonant frequency can be measured at any of the harmonic resonances. Then the phase velocity is simply given by

$$v = \frac{Lf_n}{n} \qquad \text{(ring)} \tag{5-2}$$

and

$$v = \frac{2Lf_n}{n} \qquad \text{(straight line)} \tag{5-3}$$

where

L = length of resonator

n = harmonic number

and

f_n = resonant frequency for n^{th} harmonic .

The results of velocity measurements along with theoretical curves are shown in Fig. 16 for a 50-ohm microstrip line deposited by vacuum-deposition techniques onto a very commonly used magnesium titanate substrate. The dielectric constant of a sample of this material was accurately measured by Courtney[38] of the M. I. T. Lincoln Laboratory, using a precise TE_{01} cavity technique. Since the substrate's dielectric constant was large and its thickness small, no significant fringing at the end of the straight-line resonator would be expected.[25] However, as a check, two different lengths of line were used in the measurement and the velocities compared. Negligible difference was observed. In comparing the above results with the theory, there is extremely good agreement if Maxwell's current distribution is used in the integral Eq. (2-27). The other distribution [Eq. (2-28)] produces an inaccuracy of only about 0.3 percent, while requiring one-fifth as much computer time as Maxwell's function.

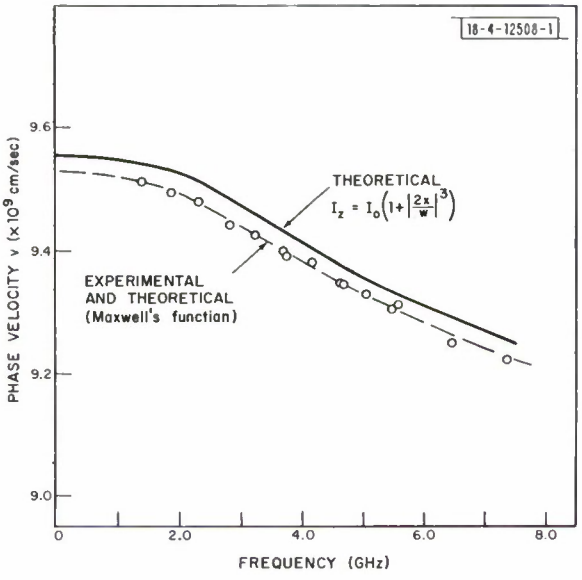

Fig. 16. Theoretical and experimental curves of phase velocity versus frequency: K = 15.87, w/d = 0.543, d = 0.1016 cm.

Using the values of effective dielectric constant versus frequency obtained from the above calculations, Eqs. (2-34) and (2-35) were used to get the variation of characteristic impedance with frequency. Negligible difference was observed between the results of these two equations. The theoretical curve is given in Fig. 17 and shows a total impedance change of only 3 percent at 8 GHz.

B. Single Microstrip Line on a Demagnetized Ferrite Substrate

For the demagnetized ferrite case, integral Eq. (2-27) is again used to obtain $\xi = \mu_{eff}\epsilon_{eff}$. The expression for the ferrite's scalar permeability, which must be substituted into the integral

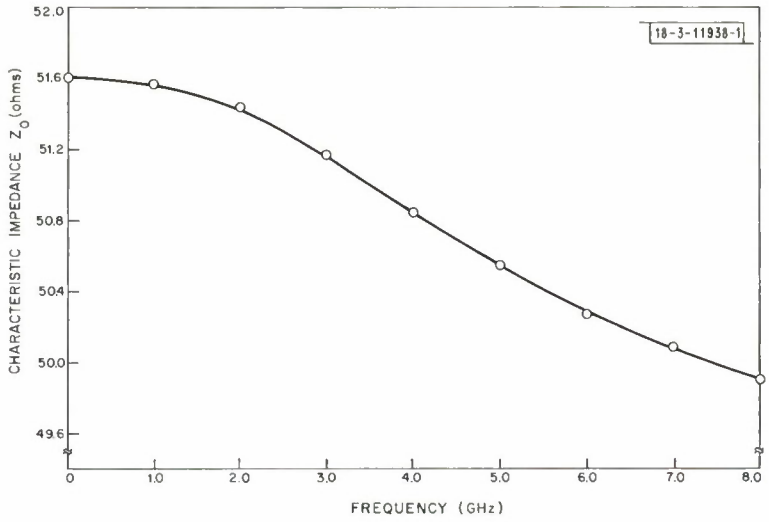

Fig. 17. Characteristic impedance versus frequency: K = 15.87, w/d = 0.543, d = 0.1016 cm.

equation, is a function of the material's saturation magnetization $4\pi M_s$ (in kG) and the frequency[36] f (in GHz),

$$\mu_r = \frac{2}{3}(1 - m_s^2)^{1/2} + \frac{1}{3} \tag{5-4}$$

where m_s is known as the normalized saturation magnetization and is given by

$$m_s = \frac{2.8(4\pi M_s)}{f}$$

with the factor 2.8 being the gyromagnetic ratio in units of GHz/kG. With the use of Eq. (2-20), a theoretical curve of ferrite microstrip phase velocity versus frequency can be obtained with $4\pi M_s$, K, w/d, and d as parameters. Figure 18 shows such a curve for a microstrip on a

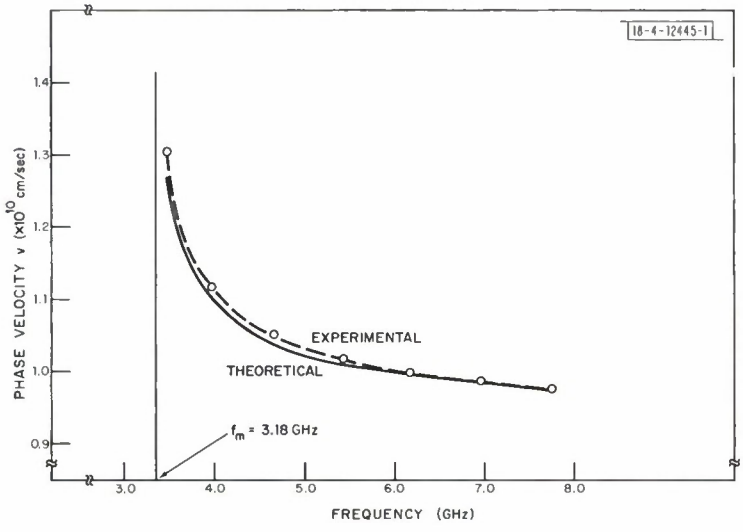

Fig. 18. Demagnetized ferrite microstrip phase velocity versus frequency: K = 15.5, w/d = 0.431, d = 0.074 cm, $4\pi M_s$ = 1.210 kG.

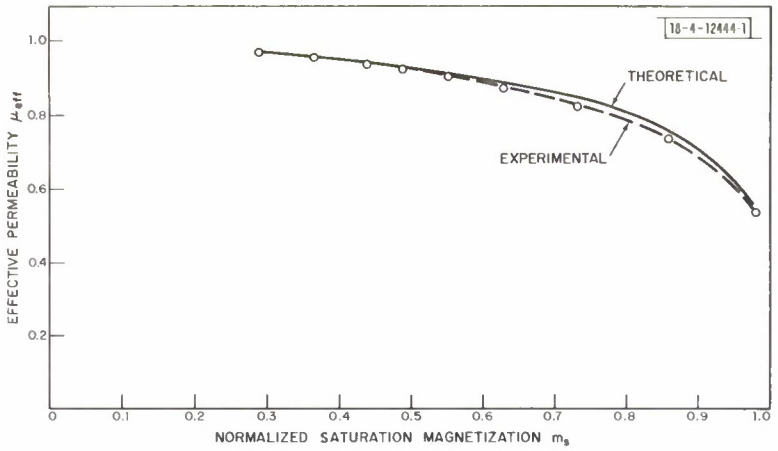

Fig. 19. Demagnetized ferrite microstrip effective permeobility versus normalized saturation magnetizotion: K = 15.5, w/d = 0.431, d = 0.074 cm, $4\pi M_s$ = 1.210 kG.

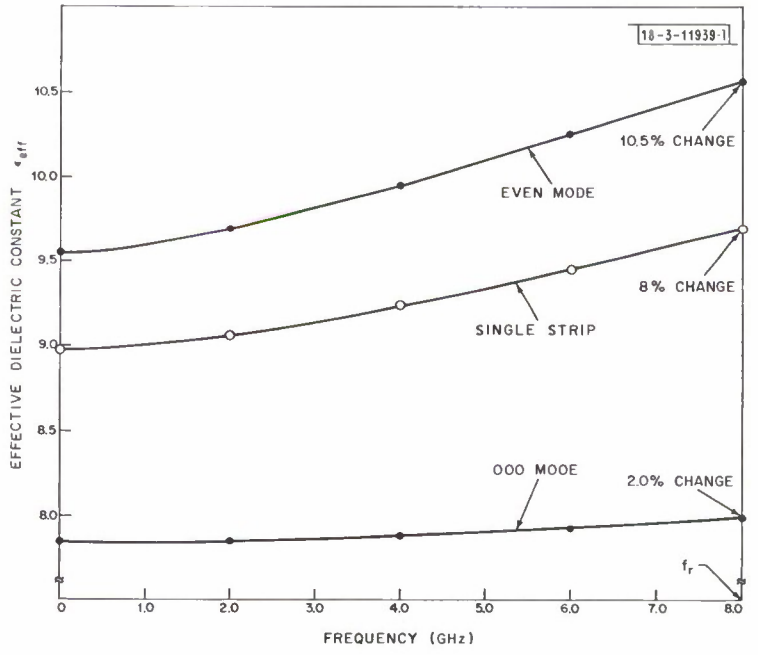

Fig. 20. Effective dielectric constant versus frequency for a coupled pair of microstrip lines on a thin substrate:

$$\text{coupled strip} \left\{ \begin{array}{l} k = 14.4 \\ w/d = 0.5 \\ d = 0.1016 \\ s/d = 0.2 \end{array} \right\} \text{single strip}$$

garnet substrate. As the permeability of the material decreases rapidly near the natural resonant frequency, $f_m = 2.8(4\pi M_s)$, the phase velocity increases at a fast rate. Experimental measurements obtained with a ring resonator given in the same figure show good agreement with the theoretical results.

A curve that is universally true for all ferrite substrate materials is that of effective permeability μ_{eff} versus normalized saturation magnetization m_s. Such a curve can be derived by using the quantity calculated above as well as an ϵ_{eff} that is a solution of the integral equation for a pure dielectric substrate having the same values of K, w/d, and d as the ferrite. Then μ_{eff} will be simply given by

$$\mu_{eff} = \frac{\xi}{\epsilon_{eff}\Big|_{dielectric}} \quad . \tag{5-5}$$

Figure 19 shows the results of this calculation along with experimental values. It has been experimentally verified by the author at Lincoln Laboratory that microstrip lines with frequently used ferrite materials having saturation magnetizations between 400 and 1400 gauss obey this same μ_{eff} vs m_s curve.

C. Coupled Pair of Microstrip Lines on a Pure Dielectric Substrate

Using the theory described in Sec. IV-C, the zero frequency values of even- and odd-mode effective dielectric constants were calculated and were found to agree within 1 percent of the coupled strip results of Bryant and Weiss.[16] This agreement is expected since the static current distribution data is used directly instead of using an approximate current distribution function as for the single strip problem. The only discrepancy might arise in the case of very narrow strips ($w/d < 0.3$), for which the discrete Fourier transform of a small number of current elements is not accurate enough. This can be remedied by making a finer grid than that chosen by Bryant and Weiss ($\Delta x/d = 0.025$).

Figure 20 shows the effect of frequency on the even- and odd-mode effective dielectric constants. The percentage change at 8 GHz for the even mode is more than five times that for the odd mode, and it has 2.5 percent more dispersion than a single microstrip line with the same parameters of K, w/d, and d. The latter calculation was made using Maxwell's current function, which is the most accurate for a w/d ratio of 0.5. Figure 21 illustrates the effect of substrate thickness on the dispersion. This curve is given for a value of d which is three times that for the previous curve, but otherwise has the same microstrip parameters. An important conclusion can be drawn from the two curves. If only the parameter d is changed by a ratio d_1/d_2, then the resulting percentage changes of the effective dielectric constant from the static value are approximately related by this same ratio. The latter can also be expressed in terms of the divergence frequency given by Eq. (5-1). This conclusion is summarized in the following manner:

$$\frac{\left\{\Delta\epsilon_{eff}\Big|_{d_1, f}\right\}\%}{\left\{\Delta\epsilon_{eff}\Big|_{d_2, f}\right\}\%} = \frac{f_{c2}}{f_{c1}} = \frac{d_1}{d_2} \quad . \tag{5-6}$$

If the substrate dielectric constant should also be changed, then the divergence frequency ratio can again be used as

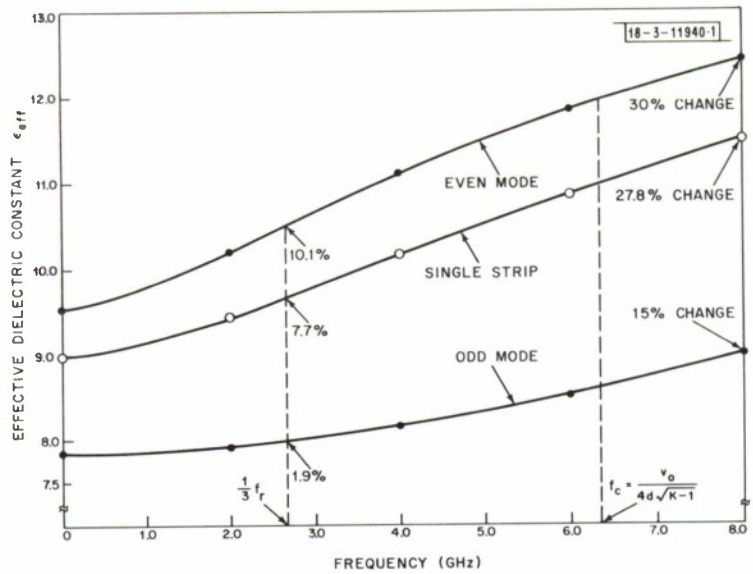

Fig.21. Effective dielectric constant versus frequency for a coupled pair of microstrip lines on a thick substrate: K = 14.4, w/d = 0.5, s/d = 0.2, d = 0.3048 cm.

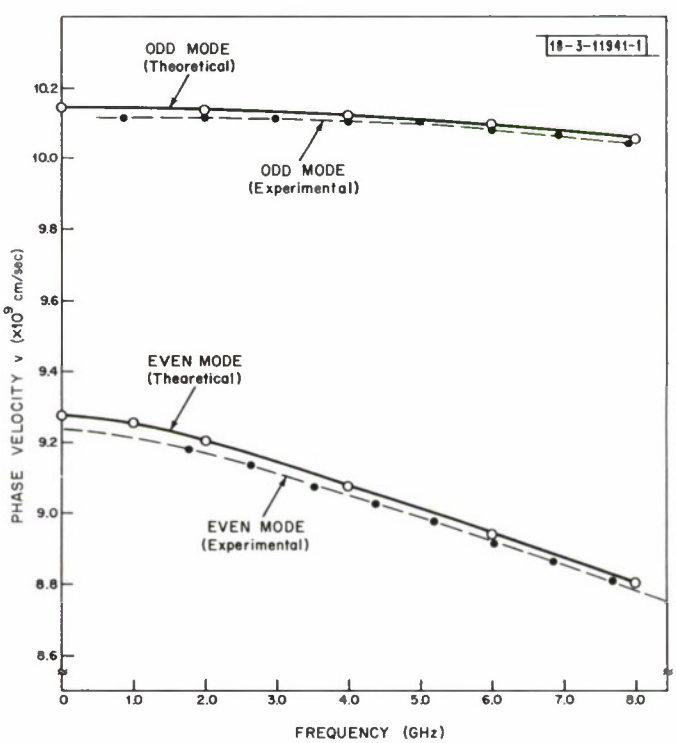

Fig.22. Theoretical and experimental curves of even- and odd-mode phase velocity versus frequency for coupled lines: K = 16.24, w/d = 0.375, s/d = 0.25, d = 0.1041 cm.

$$\frac{\left\{\Delta\epsilon_{eff}\Big|_{d_1, K_1, f}\right\}\%}{\left\{\Delta\epsilon_{eff}\Big|_{d_2, K_2, f}\right\}\%} = \frac{f_{c2}}{f_{c1}} = \frac{d_1\sqrt{K_1 - 1}}{d_2\sqrt{K_2 - 1}} \quad . \tag{5-7}$$

Of course, for both of these relationships to hold, the parameters of w/d and s/d for the even- and odd-mode calculations and w/d for the single strip must remain constant. However, it has been observed that the strip width and gap spacing have much less effect on the amount of dispersion than does the substrate's thickness and dielectric constant. Therefore, an approximation of the effective dielectric constant for any set of microstrip parameters can be obtained by using the frequency dependence given in Fig. 21 and the static values of effective dielectric constant given by Bryant and Weiss[16]:

$$\epsilon_{eff}(f) = \epsilon_{eff}(0) + \frac{f_c}{f'_c}\,\delta'(f) \tag{5-8}$$

where

f_c = divergence frequency for the desired microstrip line

$= v_o/4d\sqrt{K - 1}$

$\epsilon_{eff}(0)$ = static value of effective dielectric constant given by Bryant and Weiss for the desired microstrip line

$\delta'(f) = \dfrac{\epsilon'_{eff}(f) - \epsilon'_{eff}(0)}{\epsilon'_{eff}(0)}$ for parameters given in Fig. 21

and

f'_c = divergence frequency in Fig. 21 = 6.35 GHz .

It must be pointed out that the above formulas are only rough approximations. In reality, the even and odd modes and the single microstrip mode all have different inflection points for their dispersion curves because of their different degrees of dielectric loading. The inflection point f_c shown in Fig. 21 applies only to the single microstrip line. It is evident from the shapes of the curves in this figure that the even mode's inflection point is lowest, the single line point is a little further out on the frequency axis, and the odd-mode point is much further out and is the highest of the three. Thus, Eq. (5-8) is most accurate for the even mode and the single strip effective dielectric constants.

Figure 22 gives a comparison between theoretical and experimental curves of phase velocity versus frequency for coupled lines on a magnesium titanate substrate. The disagreement is less than 0.5 percent over the entire frequency range of 1.0 to 8.0 GHz.

D. Coupled Pair of Microstrip Lines on a Demagnetized Ferrite Substrate

For coupled lines on a demagnetized ferrite substrate, the same procedure as for the pure dielectric substrate is followed. Schlömann's[36] expression for permeability [Eq. (5-4)] is used in the integral equation for obtaining $\xi = \mu_{eff}\epsilon_{eff}$ and the phase velocity $v = v_o/\sqrt{\xi}$.

Curves of phase velocity versus frequency for a typical garnet material (composed of aluminum-gadolinium-substituted yttrium iron garnet) having the same microstrip parameters

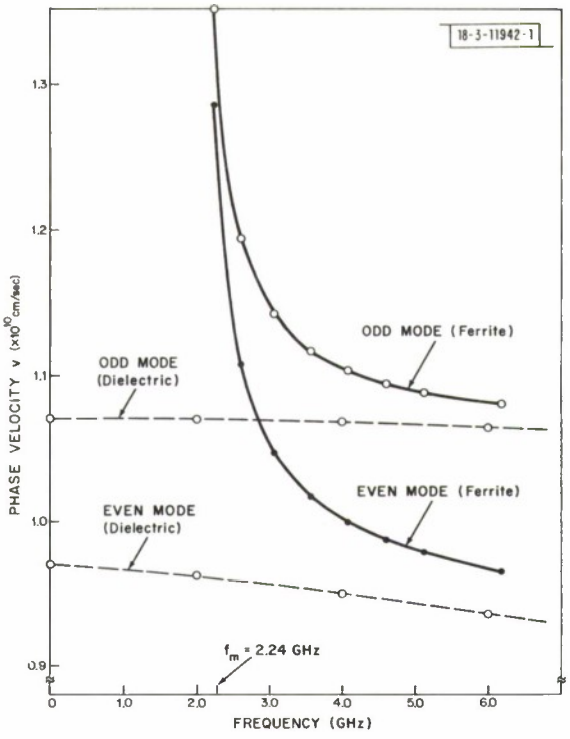

Fig.23. Phose velocity versus frequency for coupled lines on o demagnetized ferrite substrate: K = 14.4, w/d = 0.5, s/d = 0.2, d = 0.1016 cm, $4\pi M_s$ = 0.800 kG.

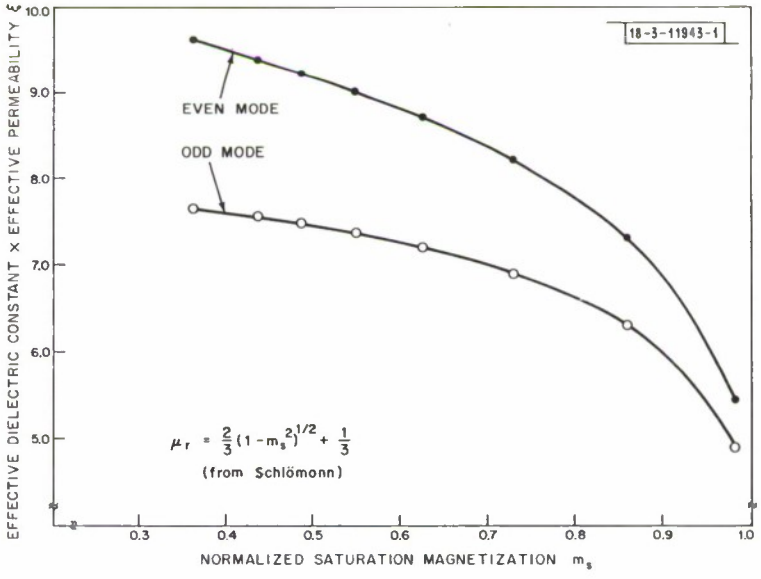

Fig.24. Product of effective dielectric constant and effective permeability (μ_{eff}) versus normalized soturotion mognetization (m_s) for coupled lines on a demagnetized ferrite substrate: K = 14.4, w/d = 0.5, s/d = 0.2, d = 0.1016 cm.

of K, w/d, s/d, and d as those used in Sec. V-C, are shown in Fig. 23. For comparison, the even- and odd-mode velocity curves for a pure dielectric with identical relative dielectric constant, K = 14.4, are also shown. At high frequencies, the ferrite curves asymptotically approach those for the dielectric. However, near the natural resonant frequency, they are quite different since at this point, the ferrite microstrip even- and odd-mode phase velocities increase rapidly as the material's permeability becomes small. The important thing to note here is that over a wide frequency band, the even- and odd-mode phase velocities for coupled lines on ferrite are closer together than those on pure dielectric. This should make ferrite a very attractive substrate material to use for microstrip directional couplers. The reason for this has already been discussed in Sec. IV-E.

Curves that are applicable to all ferrite materials with the same dielectric constant are shown in Figs. 24 and 25. The former shows how the propagation constants for the two modes approach one another as the normalized saturation magnetization m_s is varied between 0.4 and 1.0. By judicious choice of ferrite material,[36] operation with reasonable losses is limited to the region $m_s \leqslant 0.85$. For $m_s > 0.85$, the ferrite's natural resonance causes the material to be exceedingly lossy. Figure 25 shows curves of effective permeability versus normalized saturation magnetization. Note the very small difference between the values for the even mode and for the single strip, while the odd-mode values are somewhat higher and become increasingly different as $m_s = 1.0$ is approached. The odd mode exhibits a higher effective permeability for the simple reason that more of its fields extend into the air region above the surface of the microstrip substrate.

The advantage of using ferrite for couplers was demonstrated by comparing ferrite microstrip contradirectional couplers, constructed as shown in Fig. 6, with a device having the same microstrip parameters but with a pure dielectric substrate. The parameters w/d, s/d, d, and K were those used for the theoretical curves shown in Figs. 23, 24, and 25 and were chosen to give a coupling coefficient of 9 dB.[31] With the ceramic substrate, the bandwidth over which this

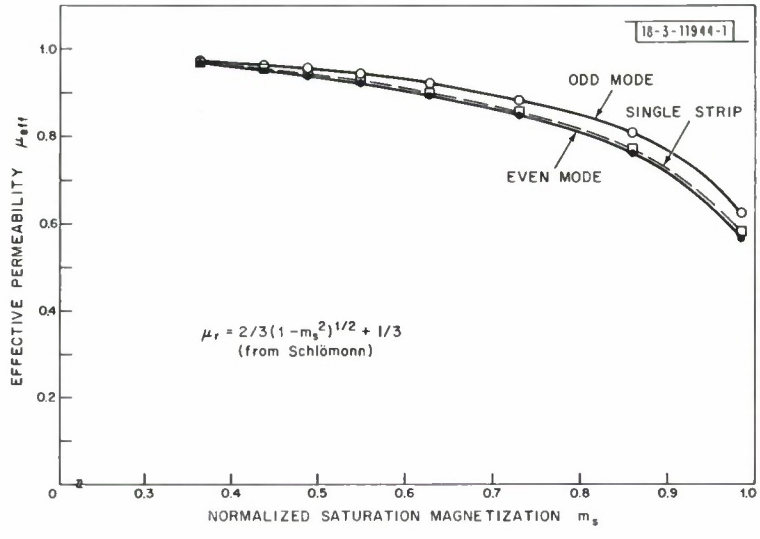

Fig. 25. Effective permeability versus normalized saturation magnetization for coupled lines on a demagnetized ferrite substrate: K = 14.4, w/d = 0.5, s/d = 0.2, d = 0.1016 cm.

coefficient remained constant was 1.2 GHz. By using a ferrite substrate, the coupling bandwidth was increased to 2.0 GHz. Also, the device's directivity was improved by at least 5 dB over the coupler's useful bandwidth. The forward loss from ports 1 to 2 did not significantly increase until the normalized saturation magnetization (m_s) exceeded 0.85. Above $m_s = 1.0$, there was more than 30 dB of loss at all of the ports.

E. Coupled Pair of Microstrip Lines on a Magnetized Ferrite Substrate with Fields Circularly Polarized

This section illustrates how nonreciprocal interaction can take place when a pair of ferrite microstrip lines, subject to a steady longitudinal magnetic field, are in a configuration which causes their RF magnetic fields to be circularly polarized. This case is discussed in Sec. IV-E in connection with a meander-line phase shifter. If the scalar permeability Eqs. (4-14) and (4-15) are used for calculating the forward and reverse propagation constants, respectively, then curves of $\xi = \mu_{eff}\epsilon_{eff}$ versus frequency are obtained, as shown in Fig. 26. These curves are for a garnet substrate, which is assumed to be latched at the remanent point of its B-H loop with $\overline{k}$ parallel to $\overline{M}$. Even- and odd-mode phase velocities can easily be obtained by using the relation $v = v_o/\sqrt{\xi}$. The values of ξ for the reverse direction are essentially the same as for a pure dielectric substrate, which indicates there is very little interaction of the fields with the ferrite. However, when the wave is propagating in the same direction as the ferrite's magnetic moments are aligned, there is strong interaction with the ferrite. This results in a large differential phase shift.

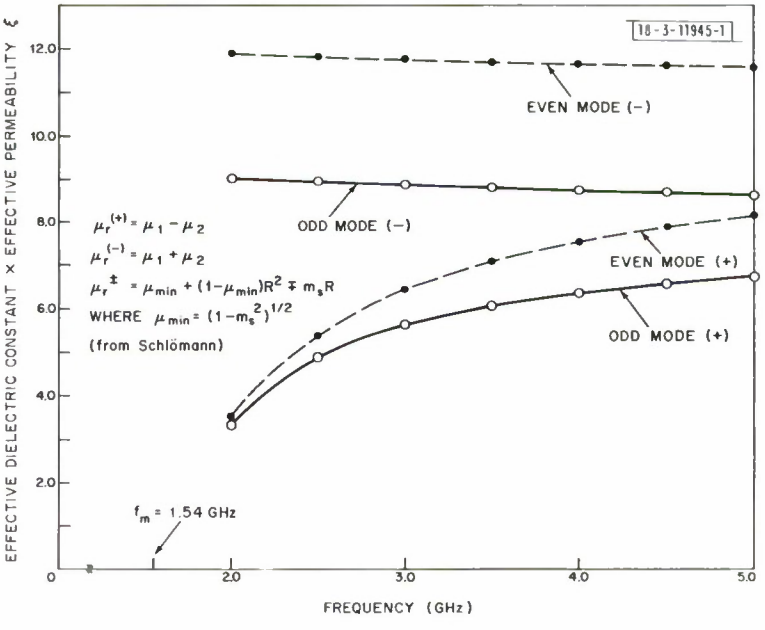

Fig. 26. Product of effective dielectric constant and effective permeability (μ_{eff}) versus frequency for coupled lines on a magnetized ferrite substrate (RF magnetic fields assumed to be circularly polarized): K = 14.4, w/d = 0.5, s/d = 0.2, d = 0.1016 cm, $4\pi M_s$ = 0.550 kG (ferrite latched in remanent state), remanence ratio = 0.7.

F. Summary

In this section, the frequency dependence of single and coupled microstrip lines was illustrated by the use of theoretical equations developed in previous sections. For microstrip with a pure dielectric substrate, the amount of frequency dispersion is primarily affected by the substrate's dielectric constant K and thickness d. However, in the case of a ferrite substrate, the normalized saturation magnetization m_s is the most important factor to consider. Agreement between theoretical and experimental results for both single and coupled microstrip was found to be very good.

When the coupled microstrip theory was applied to a quarter-wave directional coupler, the use of a ferrite substrate resulted in a significant improvement of device performance over that obtained with a ceramic substrate. Nonreciprocal interaction with coupled microstrip lines on a magnetized ferrite substrate, which is essential for meander-line phase shifter operation, was also demonstrated.

VI. CONCLUSIONS

The main contribution of this study is a frequency-dependent solution for microstrip on both a pure dielectric substrate and a ferrite substrate which exhibits gyromagnetic properties upon being magnetized. It utilizes a novel Fourier transform method that sums up the solutions for a "fictitious" surface current distribution in order to obtain the fields that are caused by the actual current distribution that is finite only over the region occupied by the conducting strip (or strips for the coupled line case). Due to the fact that the transverse current is expected to be much smaller in amplitude than the longitudinal current for normal operating frequencies and strip widths, a solution involving only the longitudinal current was found to be sufficiently accurate. This has been demonstrated by the excellent agreement obtained between theoretical and experimental values of phase velocity over a wide frequency range for both single and coupled lines on dielectric and ferrite substrates.

Some of the most interesting theoretical results obtained from the study of frequency dependent behavior of microstrip lines are: (1) the dispersion curve has an inflection point which is a function of the substrate's thickness d, dielectric constant K, and velocity of light v_o according to the equation $f_c = v_o/(4d\sqrt{K-1})$; (2) at very high frequencies, the effective dielectric constant asymptotically approaches the substrate's dielectric constant K and the phase velocity approaches $v_o/\sqrt{K}$, which indicates an increasing part of the energy is being confined to the dielectric; (3) the dispersion of the even mode in coupled microstrip lines is about five times as great as that of the odd mode and is slightly greater than that for a single microstrip line; and (4) the effective permeability of coupled microstrip on a demagnetized ferrite substrate is higher for the odd mode than for the even mode, and the values for the two modes become increasingly different as m_s approaches 1.0.

The theory presented for a coupled pair of microstrip lines is applicable to a variety of microwave integrated circuit devices. Two examples have been given here: a directional coupler and a meander-line phase shifter. An interesting result was obtained in regard to the former device. If a ferrite substrate is operated in a frequency region corresponding to normalized saturation magnetization (m_s) values greater than about 0.4, then the even- and odd-mode phase velocities become increasingly closer together as m_s approaches 1.0 and are always closer together than for the case of a pure dielectric substrate. Since the coupler's scattering matrix

predicts better performance with more equal phase velocities, the use of a ferrite substrate for this much-needed device looks very promising. Experimental data show that a significant improvement in bandwidth and directivity can be obtained by using ferrite instead of ceramics.

Much more work is required before the complete understanding of the meander-line phase shifter is achieved. It requires a knowledge of how the degree of circular polarization varies over the cross section of the device in order to theoretically predict the phase shift. Such an investigation might well result in an "effective polarization factor" that one can use in modifying the result for perfect circular polarization given in this study.

The most important investigation that is needed for the magnetized ferrite microstrip problem is that regarding the permeability of the substrate. An analysis similar to that accomplished by Schlömann for the cylindrical domain configuration must be made for obtaining the effective diagonal and off-diagonal permeability tensor components for the thin slab configuration. Once these are obtained, they can be used in the integral equation of this study for the propagation constant and phase velocity of either a single or a coupled pair of ferrite-filled microstrip lines for any degree of magnetization along the direction of propagation.

In the microstrip theory presented here, losses were completely neglected. For a ferrite substrate, the imaginary part of the permeability μ'' becomes very significant as the normalized saturation magnetization approaches unity. Thus, it is recommended that the theory be modified to include the losses of the ferrite material. This is not believed necessary for most dielectric materials since their loss tangents are usually quite low ($\tan \delta_d \cong 0.0002$).

Another factor which was neglected in this study is radiation. If the latter is included, the transverse propagation constant is no longer a real quantity but is complex. As a result, care must be taken in choosing the proper contour of integration in the complex α plane for obtaining the field quantities. Integration can no longer be taken along the real axis as was done in Eqs. (2-9) and (3-6).

It is hoped that this dynamic solution for both dielectric-filled and ferrite-filled microstrip will explain the frequently observed discrepancies between experimental results and the existing tabulated results from static solutions. Now required lengths of line such as quarter-wave matching transformers for circulators, etc., can be very accurately determined at any frequency without the use of trial and error methods.

APPENDIX A
MICROSTRIP CURRENT DISTRIBUTION

This appendix gives a derivation of the expressions of Eqs. (2-1) and (2-6) for the longitudinal and transverse components of current, respectively, and also the relative magnitude of these two components.

I. DERIVATION OF MAXWELL'S CHARGE DISTRIBUTION FUNCTION

The following derivation for the charge density distribution on an isolated conducting strip was abstracted from Maxwell.[23] For the dynamic case, it applies to the TEM solution for the longitudinal surface current distribution on a microstrip line as long as the ground plane is spaced far enough away from the strip. As shown in Sec. V-B, this restriction corresponds to keeping the w/d values less than about 1.2. Because the circuit dimensions are very small compared to a wavelength, we assume this treatment to be quasi-static in nature and thus the hybrid mode current distribution is taken to be the same as that for a pure TEM mode. This assumption is borne out by the extremely good agreement between theoretical and experimental results. Since this good agreement extends up to very high frequencies (at least 8 GHz), the skin effect, which would draw the current distribution even further to the edges of the strip with increasing frequency, must be a second order effect. The Maxwell distribution approaches infinity at the strip's edge anyway, so that the form of the distribution remains consistent with the skin effect.

Maxwell considered an isolated conducting strip, as shown in Fig. A-1, on which a charge of 1 coulomb/meter was placed. He used a conformal transformation to find how this charge distributes itself across the strip.

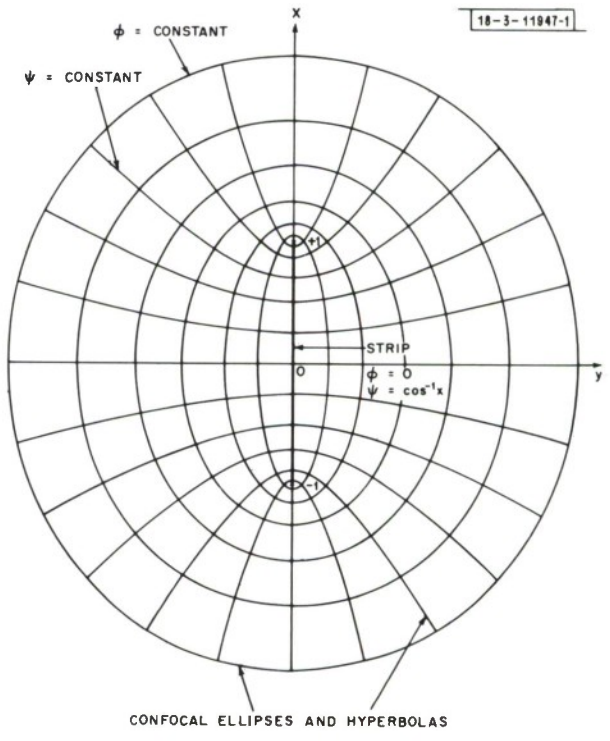

Fig. A-1. Isolated conducting strip with equipotential lines (ϕ = constant) and charge flow lines (ψ = constant).

The variables x and y were expressed as conjugate functions of the variables ϕ and ψ by summing two sets of conjugate functions:

$$x_1 = e^{\phi} \cos\psi \qquad y_1 = e^{\phi} \sin\psi$$

$$x_2 = e^{-\phi} \cos\psi \qquad y_2 = -e^{-\phi} \sin\psi$$

$$2x = x_1 + x_2 = (e^{\phi} + e^{-\phi}) \cos\psi \qquad 2y = y_1 + y_2 = (e^{\phi} - e^{-\phi}) \sin\psi \quad .$$

The points for which ϕ is constant lie on the ellipse whose axes are $e^{\phi} + e^{-\phi}$ and $e^{\phi} - e^{-\phi}$. The points for which ψ is constant lie on the hyperbola whose axes are $2\cos\psi$ and $2\sin\psi$. The x axis between $x = -1$ and $x = +1$ is accordingly described by

$$\phi = 0 \quad , \quad \psi = \cos^{-1} x \quad . \tag{A-1}$$

In order to apply this analysis to the microstrip problem, we note that ϕ = constant and ψ = constant from an orthogonal family of curves. Therefore, ϕ is taken as the potential function and ψ the function of flow. The surface charge density at any point on the conducting strip is then given by

$$\sigma(x) = \frac{1}{\pi} \frac{d\psi}{dx} \qquad -1 \leqslant x \leqslant 1 \quad . \tag{A-2}$$

Substituting Eq. (A-1) into the above equation gives

$$\sigma(x) = \frac{1}{\pi \sqrt{1 - x^2}} \qquad -1 \leqslant x \leqslant 1 \quad . \tag{A-3}$$

If the strip width is w instead of 2 and the total charge on the strip is σ_o instead of 1, then the surface charge distribution becomes

$$\sigma(x) = \frac{\sigma_o}{\pi \sqrt{1 - (2x/w)^2}} \qquad -w/2 \leqslant x \leqslant w/2 \quad . \tag{A-4}$$

II. DERIVATION OF TRANSVERSE CURRENT DISTRIBUTION FUNCTION

Since the charge density varies across the width of the microstrip line and the phase velocity in the substrate is different from that in the air, a transverse component of current is never identically zero. The following analysis uses the equation of continuity and the previously derived charge density distribution function to obtain an approximate expression for this x component of surface current I_x. It is assumed that there is much less spatial variation of the longitudinal current with z as there is variation of the transverse current with x. This is to say that the strip width is assumed to be much less than a wavelength.

Consider an incremental area S in the center of the strip, as shown in Fig. A-2. Both longitudinal and transverse surface currents are assumed to flow on the strip which has a surface charge density given by Eq. (A-4). The equation of continuity relating the total vector surface current I to the above quantity σ is

$$\nabla \cdot \overline{I} = -\frac{\partial \sigma}{\partial t} \quad . \tag{A-5}$$

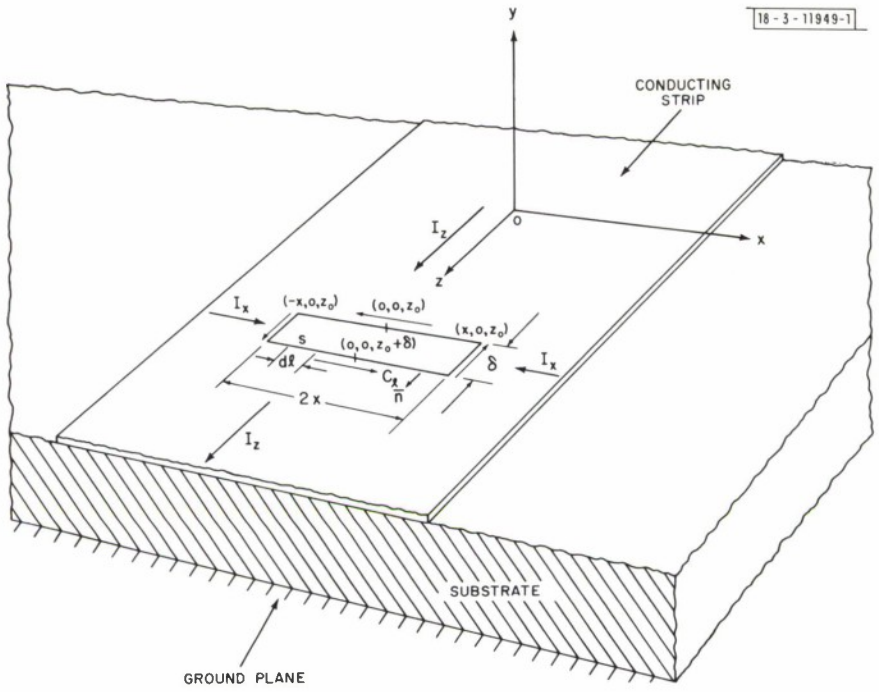

Fig. A-2. Surface currents on the conducting strip of the microstrip configuration.

This equation can also be expressed in integral form by

$$\oint_{C_\ell} \bar{I} \cdot \bar{n} d\ell = -\int_S \frac{\partial \sigma}{\partial t} dS \tag{A-6}$$

where C_ℓ is the curve enclosing area S, $d\ell$ is an incremental distance along this curve, and $\bar{n}$ is an outward normal vector to the curve. Assume that σ and I vary as $e^{j(\omega t - kz)}$ and that δ is infinitesimally small. Then the above continuity equation becomes

$$e^{-jkz_o}[2xI_z - \delta I_x - 2xI_z - \delta I_x] = -j\omega \int_{z_o}^{z_o+\delta} \int_{-x}^{x} \sigma(x)\, e^{-jkz}\, dx dz$$

$$2\delta I_x e^{-jkz_o} = j\omega \int_{-x}^{x} \sigma(x) \frac{[e^{-jk(\delta+z_o)} - e^{-jkz_o}]}{-jk} dx$$

$$\cong j\omega\delta e^{-jkz_o} \int_{-x}^{x} \sigma(x)\, dx$$

$$I_x(x) = j\omega \int_{o}^{x} \sigma(x)\, dx \quad . \tag{A-7}$$

Substituting Eq. (A-4) into this equation gives for the transverse current distribution function

$$I_x(x) = -j\omega \frac{\sigma_o}{\pi} \frac{w}{2} \sin^{-1}\left(\frac{2x}{w}\right) \qquad -\frac{w}{2} < x < \frac{w}{2} \quad . \tag{A-8}$$

III. RELATIVE AMPLITUDE OF LONGITUDINAL AND TRANSVERSE CURRENTS

As shown in Secs. II and III, the dynamic solution for the microstrip transmission line is enormously simplified if one can assume that only a longitudinal current flows on the strip. The purpose of this section is to illustrate how insignificant the transverse component is relative to the longitudinal component and, therefore, to justify the above assumption.

Consider a microstrip line on a substrate whose dielectric constant is 15. According to the charge distribution data of Bryant and Weiss, the total charge on a strip which is at a potential of 1 volt is approximately 200×10^{-12} coul/m-volt. If 1 milliwatt of power P is being carried by a microstrip line with $Z_o = 50$ ohms, then the actual potential of the strip is

$$V = \sqrt{Z_o P}$$

$$\cong 0.02 \text{ volt} \quad . \tag{A-9}$$

Thus, the total charge becomes

$$\sigma_o \cong 0.02 \text{ volt} \times 200 \times 10^{-12} \text{ coul/m-volt}$$

$$\cong 4.0 \times 10^{-12} \text{ coul/m} \quad . \tag{A-10}$$

Substituting this value of σ_o into Eq. (A-4) gives

$$\sigma(x) = \frac{1.3 \times 10^{-12}}{\sqrt{1 - (2x/w)^2}} \quad . \tag{A-11}$$

The surface current on the strip is related to the above charge function by

$$I_z(x) = v\sigma(x) = \frac{1.3 \times 10^{-4}}{\sqrt{1 - (2x/w)^2}} \text{ coul/sec} \tag{A-12}$$

where v = phase velocity $\approx 1 \times 10^8$ m/sec. Then the total longitudinal current is approximately

$$I_{zo} = v\sigma_o$$

$$= 4.0 \times 10^{-4} \text{ coul/sec} \quad . \tag{A-13}$$

In order to get the approximate amplitude of the transverse current, the continuity Eq. (2-5) relating $\sigma(x)$ and $I_x(x)$ gives

$$I_x(x) = -j\omega \int_o^x \sigma(x)\, dx \quad . \tag{A-14}$$

Substituting Eq. (A-11) into this equation results in the transverse current distribution function

$$I_x(x) = -j(1.3 \times 10^{-12})\, \omega\, \frac{w}{2} \sin^{-1}(2x/w) \text{ coul/sec} \quad . \tag{A-15}$$

Notice that this current function is directly proportional to the angular frequency $\omega = 2\pi f'$ and the strip width w. Averaging the function over half the strip width gives the approximate amplitude

$$I_{xo} = \frac{1}{w/2} \int_{o}^{w/2} I_x(x)\, dx$$

$$|I_{xo}| = (0.37 \times 10^{-12})\, \omega w \quad . \tag{A-16}$$

Typical values of frequency and strip width are

$$f = \frac{\omega}{2\pi} = 3\,\text{GHz}$$

$$w = 5 \times 10^{-4}\,\text{m} \quad .$$

Using these values, the magnitude of the transverse current is

$$|I_{xo}| = 0.035 \times 10^{-14}\,\text{coul/sec} \quad . \tag{A-17}$$

Comparing this with the amplitude of the longitudinal current given by Eq. (A-13) results in a ratio

$$\left|\frac{I_{xo}}{I_{zo}}\right| \cong 0.009 \quad . \tag{A-18}$$

Thus, for typical operating frequencies and strip widths, the transverse current amplitude is on the order of 1 percent of the longitudinal current amplitude.

APPENDIX B
COEFFICIENTS OF HERTZIAN POTENTIALS FOR MICROSTRIP ON A DIELECTRIC OR DEMAGNETIZED FERRITE SUBSTRATE

This appendix derives expressions for the coefficients of the potential functions given by Eq. (2-13) in Sec. II. Once these coefficients are known, then all the field quantities can be obtained by using the relationship for the Hertzian potentials and Eqs. (2-12).

Expanding matrix Eq. (2-19) into four equations gives

$$a_{11}A_s + a_{12}B_s + 0 + 0 = 0 \tag{B-1}$$

$$0 + 0 + a_{23}C_s + a_{24}D_s = -jkI_x(\alpha)/P_2^2 \tag{B-2}$$

$$a_{31}A_s + a_{32}B_s + a_{33}C_s + a_{34}D_s = 0 \tag{B-3}$$

and

$$a_{41}A_s + a_{42}B_s + a_{43}C_s + a_{44}D_s = I_z(\alpha) \quad . \tag{B-4}$$

Solving these equations simultaneously for the coefficients A_s, B_s, C_s, and D_s results in

$$A_s = (P_2/P_1)^2 \, B_s/\sin\beta_1 d \tag{B-5}$$

$$C_s = (P_2/P_1)^2 \, D_s/\cos\beta_1 d - jkI_x(\alpha)/P_1^2 \cos\beta_1 d \tag{B-6}$$

$$B_s = \frac{jI_x(\alpha)\left[\dfrac{\omega\mu_r\mu_o\beta_1 \tan\beta_1 d}{P_1^2} b_{22} + \dfrac{k\alpha}{P_1^2} b_{12}\right] - I_z(\alpha)\, b_{12}}{\mathrm{Det}(b_{ij})} \tag{B-7}$$

and

$$D_s = \frac{-jI_x(\alpha)\left[\dfrac{k\alpha}{P_1^2} b_{11} - \dfrac{\omega\mu_r\mu_o\beta_1 \tan\beta_1 d}{P_1^2} b_{21}\right] + I_z(\alpha)\, b_{11}}{\mathrm{Det}(b_{ij})} \tag{B-8}$$

where

$$\mathrm{Det}(b_{ij}) = b_{11}b_{22} - b_{12}b_{21}$$

$$b_{11} = -b_{22} = \alpha\left[\left(\frac{P_2}{P_1}\right)^2 - 1\right]$$

$$b_{12} = \frac{\omega\mu_o\beta_1}{k}\left[\left(\frac{P_2}{P_1}\right)^2 \mu_r \tan\beta_1 d - \frac{\beta_2}{\beta_1}\right]$$

and

$$b_{21} = \frac{\omega K\epsilon_o\beta_1}{k}\left[\left(\frac{P_2}{P_1}\right)^2 \cot\beta_1 d + \frac{1}{K}\frac{\beta_2}{\beta_1}\right] \quad .$$

For the analysis which includes only the longitudinal component of current, set $I_x(\alpha)$ equal to zero in the above equations for the coefficients.

APPENDIX C
COEFFICIENTS OF HERTZIAN POTENTIALS FOR MICROSTRIP ON A MAGNETIZED FERRITE SUBSTRATE

I. COMPLETE SOLUTION

The complete solution that includes all the propagating modes supported by the ferrite-filled microstrip line has six Hertzian potential coefficients. Four of these can be obtained by solving the set of simultaneous Eqs. (3-24), given in Sec. III. The remaining two coefficients A_t and C_t are obtained from boundary conditions (3-17) and (3-18). All the electromagnetic field quantities can then be obtained by using Eqs. (3-11), (3-12), (3-13), (3-15), and (3-16).

The potential coefficients needed for obtaining the propagation constant are given by

$$G_t = -Z_1 I_z(\alpha) + Z_2 I_x(\alpha)$$

$$F_t = Z_3 I_z(\alpha) - Z_4 I_x(\alpha)$$

where

$$Z_1 = \frac{1}{\mathrm{Det}(a_{ij})} \begin{vmatrix} a_{11} & a_{12} & 0 \\ a_{21} & a_{22} & a_{24} \\ a_{31} & a_{32} & a_{34} \end{vmatrix} \quad ; \quad Z_2 = \frac{1}{\mathrm{Det}(a_{ij})} \begin{vmatrix} a_{11} & a_{12} & 0 \\ a_{31} & a_{32} & a_{34} \\ a_{41} & a_{42} & a_{44} \end{vmatrix} \quad ;$$

$$Z_3 = \frac{1}{\mathrm{Det}(a_{ij})} \begin{vmatrix} a_{11} & a_{12} & a_{13} \\ a_{21} & a_{22} & 0 \\ a_{31} & a_{32} & a_{33} \end{vmatrix} \quad \text{and} \quad Z_4 = \frac{1}{\mathrm{Det}(a_{ij})} \begin{vmatrix} a_{11} & a_{12} & a_{13} \\ a_{31} & a_{32} & a_{33} \\ a_{41} & a_{42} & a_{43} \end{vmatrix} \quad .$$

The rest of the coefficients are expressed in terms of F_t and G_t by the relationships

$$B_t = \frac{a_{12}[a_{24}F_t + I_x(\alpha)] - a_{13}a_{22}G_t}{a_{11}a_{22} - a_{21}a_{12}}$$

$$D_t = \frac{a_{13}a_{21}G_t - a_{11}[a_{24}F_t + I_x(\alpha)]}{a_{11}a_{22} - a_{21}a_{12}}$$

$$C_t = -(\chi_{2F}/\chi_{1F})^2 D_t$$

and

$$A_t = -\frac{\beta_{2F}T_{2F}}{\beta_{1F}T_{1F}} (\chi_{2F}/\chi_{1F})^2 B_t \quad .$$

The coefficients a_{ij} are:

$$a_{11} = b_o(S2 - b_3 S1) \quad , \quad a_{12} = b_o(C2 - C1) \quad , \quad a_{13} = a_{24} = -\frac{P_2^2}{jk}$$

$$a_{21} = b_1\left(S2 - \frac{\beta_{2F}}{\beta_{1F}} S1\right) \quad , \quad a_{22} = b_1\left(C2 - \frac{T_{1F}}{T_{2F}} C1\right)$$

$$a_{31} = \alpha S_F [b_3(\chi_{2F}/\chi_{1F})^2 S1 - S2] + \beta_{2F} T_{2F} b_2$$

$$a_{32} = -\alpha S_F b_2 + \beta_{2F} T_{2F} \left[\frac{1}{b_3} (\chi_{2F}/\chi_{1F})^2 S1 - S2\right]$$

$$a_{33} = a_{44} = j\alpha \quad , \quad a_{34} = \frac{\omega\mu_o}{k} \beta_2 \quad , \quad a_{43} = \frac{\omega\epsilon_o}{k} \beta_2$$

$$a_{41} = jk \left\{\alpha [M_{2F} S2 - b_3(\chi_{2F}/\chi_{1F})^2 M_{1F} S1] + N_F \beta_{2F} \left[\frac{T_{2F}}{T_{1F}} \left(\frac{\chi_{2F}}{\chi_{1F}}\right)^2 C1 - C2\right]\right\}$$

and

$$a_{42} = jk \left\{\alpha [M_{2F} C2 - (\chi_{2F}/\chi_{1F})^2 M_{1F} C1] + N_F \beta_{2F} \left[S2 - \frac{\beta_{1F}}{\beta_{2F}} \left(\frac{\chi_{2F}}{\chi_{1F}}\right)^2 S1\right]\right\}$$

where

$$b_o = -k \frac{\mu_2}{\mu_1} \chi_{2F}^2 \quad , \quad b_1 = j \frac{\chi_{2F}^2 T_{2F}}{k_o \mu_z} \quad , \quad b_2 = C2 - \left(\frac{\chi_{2F}}{\chi_{1F}}\right)^2 C1$$

$$b_3 = \frac{\beta_{2F} T_{2F}}{\beta_{1F} T_{1F}} \quad , \quad S1 = \sin(\beta_{1F} d) \quad , \quad S2 = \sin(\beta_{2F} d)$$

$$C1 = \cos(\beta_{1F} d) \quad \text{and} \quad C2 = \cos(\beta_{2F} d) \quad .$$

APPENDIX D
SCATTERING MATRIX FOR A MICROSTRIP DIRECTIONAL COUPLER

The scattering matrix for a quarter-wave microstrip directional coupler, which has all its ports connected to lines of characteristic impedance Z_o and is shown in Fig. 4-3, is of the form given by Eq. (4-7). By following a procedure similar to that of Jones and Bolljahn,[34] Thomas Bryant of Lincoln Laboratory derived the following expressions for the matrix elements from which the coupler's forward loss, coupling coefficient, isolation, and input reflection coefficient can be determined:

$$B_c = \frac{1}{DEN}\left\{2(D_e \cos\theta_e + D_o \cos\theta_o) + j(A_3 D_e \tan\theta_o \cos\theta_e + A_1 D_o \tan\theta_e \cos\theta_o)\right\}$$

$$C_c = \frac{1}{DEN}\left\{(Z'_{oo}A_1 - Z'_{oe}A_3)\tan\theta_e \tan\theta_o + j(A_2 \tan\theta_e + A_4 \tan\theta_o)\right\}$$

$$D_c = \frac{1}{DEN}\left\{2(D_e \cos\theta_e - D_o \cos\theta_o) + j(A_3 D_e \tan\theta_o \cos\theta_e - A_1 D_o \tan\theta_e \cos\theta_o)\right\}$$

By using the power-conservation condition for a lossless junction,[39] the matrix element A_c can be found from the following relations:

$$|A_c| = \sqrt{1 - |B_c|^2 - |C_c|^2 - |D_c|^2}$$

$$\phi_A = \phi_B - \cos^{-1}\left\{-\frac{|C_c|\,|D_c|}{|B_c|\,|A_c|}\cos(\phi_C - \phi_D)\right\}$$

where

$$Z'_{oo} = \frac{Z_{oo}}{Z_o} \qquad Z'_{oe} = \frac{Z_{oe}}{Z_o}$$

$$\theta_o = \frac{\omega}{v_{od}}\ell \qquad \theta_e = \frac{\omega}{v_{ev}}\ell$$

$$A_1 = Z'_{oe} + \frac{1}{Z'_{oe}} \qquad A_2 = Z'_{oe} - \frac{1}{Z'_{oe}}$$

$$A_3 = \frac{1}{Z'_{oo}} + Z'_{oo} \qquad A_4 = \frac{1}{Z'_{oo}} - Z'_{oo}$$

$$D_o = 1 + \tan^2\theta_o \qquad D_e = 1 + \tan^2\theta_e$$

$$DEN = 4 - (A_1 Z'_{oo} + A_3 Z'_{oe})\tan\theta_e \tan\theta_o + j\left[\left(3Z'_{oe} + \frac{1}{Z'_{oe}}\right)\tan\theta_e + \left(3Z'_{oo} + \frac{1}{Z'_{oo}}\right)\tan\theta_o\right]$$

and

$\{\phi_A, \phi_B, \phi_C, \phi_D\}$ = phase angles of matrix elements .

The coupler's transmission losses (in dB) and reflection coefficient are given by

$$\text{Forward loss (1-2)} = 10 \log_{10} |B_c|^2$$

$$\text{Coupling (1-3)} = 10 \log_{10} |C_c|^2$$

$$\text{Isolation (1-4)} = 10 \log_{10} |D_c|^2$$

$$\text{Directivity} = 10 \log_{10} \frac{|D_c|^2}{|C_c|^2}$$

and

$$\text{Reflection Coefficient} = |A_c| \quad .$$

APPENDIX E
COMPUTER PROGRAMS

This appendix consists of computer programs that are written in Fortran IV language for the IBM-360 computer. The results of the numerical computations are described in Sec. V. Section I below lists an entire program, while the remaining sections give modifications of that program. The Fortran symbols used in this appendix are given below.

	Fortran IV Symbol
d	D
K	E1
f	F
R	RR
$4\pi M_s$	SATM
m_s	SATMN
s/d	SD
ξ	SQ or PSI
μ_r	U1
μ_{min}	UMIN
w/d	WD
value of integral	XINT
$\gamma/0.2\pi$	XN
discrete current distribution used as input data for coupled strip solution	DIST
input parameter to denote either odd mode (I = 1) or even mode (I = 2)	I

I. PROGRAM TO COMPUTE ξ FOR DIELECTRIC-FILLED MICROSTRIP

The following is a program that computes the effective dielectric constant for a single microstrip line on a pure dielectric substrate by the use of Eq. (2-27) and the current Fourier transform, given by Eq. (2-28). A flow chart of the program, which consists of five parts, is shown in Fig. E-1. The first, shown in Fig. E-2, is a general program that coordinates all the remaining subprograms and subroutines. Figure E-3 shows the next subprogram, which sums the integrand FN(XN, SQ) over values of XN ranging from 0 to 100. The integrand is evaluated by the program listed in Fig. E-4. A root-finding subroutine consisting of a half-interval search technique is given in Fig. E-5. It finds the value of ξ that makes the left-hand side of the integral Eq. (2-27) less than 10^{-5}. Figure E-6 presents an integration subroutine that uses the trapezoidal rule.

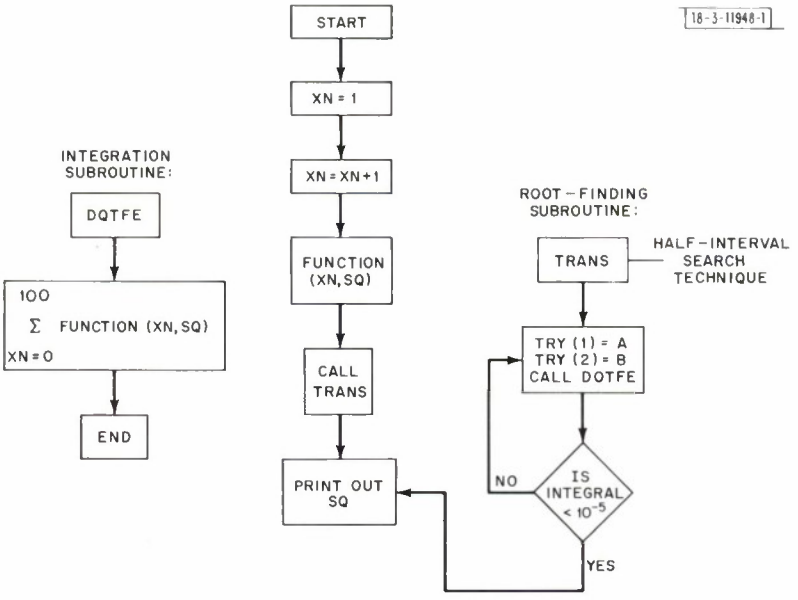

Fig.E-1. Flow chart for computer programs.

```
      IMPLICIT REAL*8 (A-H,O-Z)
      COMMON /FSUR/ U1,E1,WO,O,F,XINT
      COMMON /AM/ O1,O2,O3,D4,N1,N2,N3,N4
      OIMENSION TRY(3)
      NAMELIST /NAM1/ U1,E1,WO,O,F
      EXTERNAL SUM
      CALL CPNMON
      N1=601
      N2=301
      N3=201
      N4=101
      DO 100 JP=1,2
      WRITE(6,31)
   31 FORMAT(' U1,E1,WO,O,F' )
      READ(5,NAM1)
      TRY(1)=1.0
      TRY(2)=(E1+1.0)/2.0
      TRY(3)=E1
      D1=25./600.
      O2=25./300.
      O3=25./200.
      D4=25./100.
      LL=0
   40 LL=LL+1
      IF(LL+1.GT.3) GO TO 99
      AB=TRY(LL)+.01
      AE=TRY(LL+1)-.01
      EPS=.00001
      CALL TRANS(AB,AE,EPS,ROOT,SUM,IER)
      IF(IER.NE.0) GO TO 40
      SQ=ROOT
      WRITE(6,NAM1)
      WRITE(6,38) SQ,XINT
   38 FORMAT(/' PSI=',E12.5,'  VALUE OF INTEGRAL=',E12.5/)
      GO TO 100
   99 WRITE(6,39)
   39 FORMAT(' ROOT TROUBLE')
      GO TO 12
  100 CONTINUE
   12 CALL EXIT
      ENO
```

Fig.E-2. General program.

-3-12327

```
      FUNCTION SUM(SQ)
      IMPLICIT REAL*8 (A-H,O-Z)
      COMMON /FSUB/ U1,E1,WD,D,F,XINT
      COMMON /AM/ D1,D2,D3,D4,N1,N2,N3,N4
      DIMENSION FF(801),Z(801)
      XB=0.0
      DO 1 J=1,N1
      XN=XB+(J-1)*D1
    1 FF(J)=FN(XN,SQ)
      CALL DQTFE(D1,FF,Z,N1)
      S1=Z(N1)
      XB=25.
      DO 2 J=1,N2
      XN=XB+(J-1)*D2
    2 FF(J)=FN(XN,SQ)
      CALL DQTFE(D2,FF,Z,N2)
      S2=Z(N2)
      XB=50.
      DO 3 J=1,N3
      XN=XB+(J-1)*D3
    3 FF(J)=FN(XN,SQ)
      CALL DQTFE(D3,FF,Z,N3)
      S3=Z(N3)
      XB=75.
      DO 4 J=1,N4
      XN=XB+(J-1)*D4
    4 FF(J)=FN(XN,SQ)
      CALL DQTFE(D4,FF,Z,N4)
      S4=Z(N4)
      XINT=S1+S2+S3+S4
      SUM=XINT
      RETURN
      END
```

Fig. E-3. Summation program.

```
      FUNCTION FN(XN,SQ)
      IMPLICIT REAL*8 (A-H,O-Z)
      COMMON /FSUB/ U1,E1,WD,D,F,XINT
      IF(XN.EQ.0) GO TO 4
      DL=D/30.
      T=U1*E1-SQ
      Q=(SQ-1.)/T
      R=(U1*E1-1.)/T
      ARG1=0.2*3.1415927*XN/WD
      ARG3=0.31415927*XN
      DTDEF=DTANH(ARG1)
      P3=193.5092066/XN**3
      P1=9.54929668/XN
      P2=60.79271019/XN**2
      A=1./XN*(P3+(P1-P3)*DCOS(ARG3)+(2.-P2)*DSIN(ARG3))
      IF(F.EQ.0.0) GO TO 44
      A1=(ARG1/(F*DL))**2
      A2=(2.*3.1415927)**2*T
      SIGN=1.
      B12=(A2-A1)
      IF(B12.LT.0.0) SIGN=-1.
      B1=DSQRT(SIGN*B12)
      Z=DTAN(F*DL*B1)
      IF(B12.LT.0.0) Z=DTANH(F*DL*B1)
      B2=DSQRT((2.*3.1415927)**2*(SQ-1.)+A1)
      PART=SIGN*(Q*U1*Z+SIGN*B2/B1)
      XNUM=A*PART*B1
      XDEN=A1*R**2+SIGN*E1/SQ*B12*PART*(Q*1./Z-1./E1*B2/B1)
      GO TO 43
   44 PART=Q*U1*DTDEF-1.0
      XNUM=1.0/XN*A*PART
      XDEN=R**2-E1/SQ*PART*(Q*1.0/DTDEF-1.0/E1)
   43 IF(XDEN.EQ.0.0) WRITE(6,42) XNUM,XDEN
   42 FORMAT(' NUM=',E12.5,' DEN=',E12.5)
      FN=XNUM/XDEN
      GO TO 5
    4 FN=0.0
    5 RETURN
      END
```

Fig. E-4. Integrand evaluation program.

```
C      FILENAME IMPLI FORTRAN                                    -3-12329
       SUBROUTINE TRANS(A,B,EPS,ROOT,FCT,IER)
C*************************************************************************
C
C      THIS SUBROUTINE SOLVES A TRANSCENDENTAL EQUATION OF ONE UNKNOWN
C      BY HALF INTERVAL SEARCH METHOD.
C
C      INPUT ARGUMENTSO
C                     A=LEFT VALUE FOR INTERVAL (ROOT GREATER THAN A)
C                     B=RIGHT VALUE FOR INTERVAL (KOOT LESS THAN B)
C                     EPS=REQUIREO ACCURACY, E.G. ERROR NO GREATER THAN
C                         .000001
C                     FCT=EXTERNAL FUNCTION SUBPROGRAM PROVIOED BY USER.
C
C      OUTPUT RETURNEOO
C                     ROOT=ANSWER RETURNEO WITH ERROR NO GREATER THAN
C                          EPS
C                     IER=0 IF ROOT FOUNO
C                     IER=1 IF ROOT NOT IN INITIAL INTERVAL
C
C*************************************************************************
C      FOR DOUBLE PRECISION CHANGE ABS TO ABS THROUGHOUT AND REMOVE
C      C IN FRONT OF THE FOLLOWINGO
       IMPLICIT REAL*8 (A-H,O-Z)
       FA=FCT(A)
       IER=0
       FB=FCT(B)
       IF(FA*FB.GT.0.) GO TO 9
       IF(OABS(FA).LE.EPS) GO TO 10
       IF(DABS(FB).LE.EPS) GO TO 11
       IK=0
  100  IK=IK+1
       X=(A+B)/2.
       IF(IK.GT.40) GO TO 20
       FX=FCT(X)
       IF(OABS(FX).LE.EPS) GO TO 20
       IF(FA*FX.LT.0.) GO TO 5
       IF(FA*FX.GT.0.) GO TO 6
    5  B=X
       FB=FX
       GO TO 100
    6  A=X
       FA=FX
       GO TO 100
    9  IER=1
   66  FORMAT(' IER= ',I4)
       GO TO 30
   10  ROOT=A
       GO TO 30
   11  ROOT=B
       GO TO 30
   20  ROOT=X
   30  RETURN
       END
```

Fig.E-5. Root-finding subroutine.

```
      SUBROUTINE DQTFE(H,Y,Z,NDIM)
      DIMENSION Y(1),Z(1)
      DOUBLE PRECISION Y,Z,H,HH,SUM1,SUM2
      SUM2=0.D0
      IF(NDIM-1) 4,3,1
    1 HH=.5D0*H
      DO 2 I=2,NDIM
      SUM1=SUM2
      SUM2=SUM2+HH*(Y(I)+Y(I-1))
    2 Z(I-1)=SUM1
    3 Z(NDIM)=SUM2
    4 RETURN
      END
```

Fig. E-6. Integration subroutine.

II. MODIFICATION FOR USE OF MAXWELL'S FUNCTION

The following is a modification of the program given in the previous section for solving integral Eq. (2-27) with the Fourier transform taken equal to that of the Maxwell current distribution function.

(a) The bracketed part of the program given in Fig. E-4 is replaced by

```
YARG3 = ARG3
N = 0
D = 0.00001
CALL BESJ(YARG3, N, YA, D, IER)
A = YA
```

Replace the second line in that same figure by

```
IMPLICIT REAL*8(A-H, O-X, Z)
```

(b) Add the Bessel function subroutine BESJ given in Fig. E-7.

III. MODIFICATION FOR COUPLED PAIR OF MICROSTRIP LINES

A discrete Fourier transform of the static current distribution is used in the integral equation for ξ. This transform is given by Eq. (4-3) in Sec. IV. Before the following coupled line program can be run, the discrete values of the static current distribution using the Green's function method of Bryant and Weiss must be obtained across the substrate's surface from the origin to the outer edge of the strip. Because of the symmetry of the coupled line configuration, only the static current distribution across one of the strips is required and is evaluated at incremental strip width elements of $\Delta x/d = 0.025$. An example of this distribution is illustrated in Table E-1. It is used as input data and designated DIST(1, K) for the odd mode and DIST(2, K) for the even mode, where K = 1, 24 since there are 24 strip-width elements from the origin $x/d = 0$ to the outer edge of the strip $x/d = s/2d + w/d$.

The following modifications of the program given in Sec. I must be made in order to solve the coupled strip problem:

(a) All the common/FSUB/statements are changed to:

```
COMMON/FSUB/DIST(2, 100), F, U1, E1, WD, SD, D, XINT, I
```

(b) The NAMELIST statement is changed to:

```
NAMELIST/NAM1/F, U1, E1, WD, SD, D
```

```
C     ...............................................................
C
C        SUBROUTINE BESJ                                    [-3-12331]
C
C        PURPOSE
C           COMPUTE THE J BESSEL FUNCTION FOR A GIVEN ARGUMENT AND ORDER
C
C        USAGE
C           CALL BESJ(X,N,BJ,D,IER)
C
C        DESCRIPTION OF PARAMETERS
C           X  -THE ARGUMENT OF THE J BESSEL FUNCTION DESIRED
C           N  -THE ORDER OF THE J BESSEL FUNCTION DESIRED
C           BJ -THE RESULTANT J BESSEL FUNCTION
C           D  -REQUIRED ACCURACY
C           IER-RESULTANT ERROR CODE WHERE
C              IER=0  NO ERROR
C              IER=1  N IS NEGATIVE
C              IER=2  X IS NEGATIVE OR ZERO
C              IER=3  REQUIRED ACCURACY NOT OBTAINED
C              IER=4  RANGE OF N COMPARED TO X NOT CORRECT (SEE REMARKS)
C
C        REMARKS
C           N MUST BE GREATER THAN OR EQUAL TO ZERO, BUT IT MUST BE
C           LESS THAN
C              20+10*X-X** 2/3   FOR X LESS THAN OR EQUAL TO 15
C              90+X/2            FOR X GREATER THAN 15
C
C        SUBROUTINES AND FUNCTION SUBPROGRAMS REQUIRED
C           NONE
C
C        METHOD
C           RECURRENCE RELATION TECHNIQUE DESCRIBED BY H. GOLDSTEIN AND
C           R.M. THALER,'RECURRENCE TECHNIQUES FOR THE CALCULATION OF
C           BESSEL FUNCTIONS',M.T.A.C.,V.13,PP.102-108 AND I.A. STEGUN
C           AND M. ABRAMOWITZ,'GENERATION OF BESSEL FUNCTIONS ON HIGH
C           SPEED COMPUTERS',M.T.A.C.,V.11,1957,PP.255-257
C
C     ...............................................................
C
      SUBROUTINE BESJ(X,N,BJ,D,IER)
C
      BJ=.0
      IF(N)10,20,20
   10 IER=1
      RETURN
   20 IF(X)30,30,31
   30 IER=2
      RETURN
   31 IF(X-15.)32,32,34
   32 NTEST=20.+10.*X-X** 2/3
      GO TO 36
   34 NTEST=90.+X/2.
   36 IF(N-NTEST)40,38,38
   38 IER=4
      RETURN
   40 IER=0
      N1=N+1
```

Fig.E-7. Bessel function subroutine.

```
      BPREV=.0                                          -3-12332
C
C     COMPUTE STARTING VALUE OF M
C
      IF(X-5.)50,60,60
   50 MA=X+6.
      GO TO 70
   60 MA=1.4*X+60./X
   70 MB=N+IFIX(X)/4+2
      MZERO=MAX0(MA,MB)
C
C     SET UPPER LIMIT OF M
C
      MMAX=NTEST
  100 DO 190 M=MZERO,MMAX,3
C
C     SET F(M),F(M-1)
C
      FM1=1.0E-28
      FM=.0
      ALPHA=.0
      IF(M-(M/2)*2)120,110,120
  110 JT=-1
      GO TO 130
  120 JT=1
  130 M2=M-2
      DO 160 K=1,M2
      MK=M-K
      BMK=2.*FLOAT(MK)*FM1/X-FM
      FM=FM1
      FM1=BMK
      IF(MK-N-1)150,140,150
  140 BJ=BMK
  150 JT=-JT
      S=1+JT
  160 ALPHA=ALPHA+BMK*S
      BMK=2.*FM1/X-FM
      IF(N)180,170,180
  170 BJ=BMK
  180 ALPHA=ALPHA+BMK
      BJ=BJ/ALPHA
      IF(ABS(BJ-BPREV)-ABS(D*BJ))200,200,190
  190 BPREV=BJ
      IER=3
  200 RETURN
      END
```

Fig.E-7. Continued.

TABLE E-1

STATIC CURRENT DISTRIBUTION DATA
FOR COUPLED PAIR OF MICROSTRIP LINES

Parameters: K = 16.0, w/d = 0.50, s/d = 0.2
m = number of elementary strip widths ($\Delta x/d = 0.025$)
from plane of symmetry at x = 0.

m	Odd Mode $I_o(m)$	Even Mode $I_e(m)$	m	Odd Mode $I_o(m)$	Even Mode $I_e(m)$
1	0	0	13	0.08819	0.04617
2	0	0	14	0.08414	0.04702
3	0	0	15	0.08130	0.04821
4	0	0	16	0.07954	0.04977
5	0.56634	0.11176	17	0.07882	0.05181
6	0.22929	0.05703	18	0.07923	0.05448
7	0.17809	0.05120	19	0.08099	0.05802
8	0.14517	0.04783	20	0.08457	0.06292
9	0.12495	0.04627	21	0.09096	0.07006
10	0.11108	0.04557	22	0.10289	0.08182
11	0.10108	0.04540	23	0.12257	0.10016
12	0.09370	0.04562	24	0.27188	0.22928

(c) Statement number 31 is changed to:

```
31 FORMAT('F, U1, E1, WD, SD, D')
```

(d) After the statement "CALL CPNMON," insert the statements:

```
READ(5, 83) (DIST(1, K), K=1, 24)
READ(5, 83) (DIST(2, K), K=1, 24)
83 FORMAT(10F8.6)
```

(e) Replace the part of the original program given by Fig. E-4 by another integrand evaluation program shown in Fig. E-8 plus an additional program TSUM, which computes the discrete Fourier transform of the current distribution and is given in Fig. E-9.

IV. MODIFICATION FOR COMPUTING THE CHARACTERISTIC IMPEDANCE

The characteristic impedance is determined by using Eq. (2-34) with input parameters the same as in Sec. I except for an additional parameter ξ, which can be calculated using the program described in Sec. I. The required modifications of this program consist of eliminating the root-finding subroutine and changing the programs given in Figs. E-2 and E-4 to those shown in Figs. E-10 and E-11, respectively.

-3-12333

```
      FUNCTION FN(XN,SQ)
      IMPLICIT REAL*8 (A-H,O-Z)
      COMMON /FSUB/ DIST(2,100),F,U1,E1,WO,SD,D,XINT,I
      IF(XN.EQ.0) GO TO 4
      DL=D/30.
      T=U1*E1-SQ
      Q=(SQ-1.)/T
      R=(U1*E1-1.)/T
      ARG1=0.2*3.1415927*XN/WD
      ARG2=0.31415927*XN*(SO/WD+1.0)
      OTDEF=DTANH(ARG1)
      A=TSUM(XN,ARG1)
      IF(I.EQ.1) F=DSIN(ARG2)
      IF(I.EQ.2) F=DCOS(ARG2)
      IF(F.EQ.0.0) GO TO 44
      A1=(ARG1/(F*DL))**2
      A2=(2.*3.1415927)**2*T
      SIGN=1.
      B12=(A2-A1)
      IF(B12.LT.0.0) SIGN=-1.
      B1=DSQRT(SIGN*B12)
      Z=DTAN(F*DL*B1)
      IF(B12.LT.0.0) Z=DTANH(F*DL*B1)
      B2=DSQRT((2.*3.1415927)**2*(SQ-1.)+A1)
      PART=SIGN*(Q*U1*Z+SIGN*B2/B1)
      XNUM=A*PART*B1*E
      XDEN=A1*R**2+SIGN*E1/SQ*B12*PART*(Q*1./Z-1./E1*B2/B1)
      GO TO 43
   44 PART=Q*U1*DTDEF-1.0
      XNUM=1.0/XN*A*PART*E
      XDEN=R**2-E1/SQ*PART*(Q*1.0/DTDEF-1.0/E1)
   43 IF(XDEN.EQ.0.0) WRITE(6,42) XNUM,XDEN
   42 FORMAT(' NUM=',E12.5,' DEN=',E12.5)
      FN=XNUM/XDEN
      GO TO 5
    4 FN=0.0
    5 RETURN
      END
```

Fig.E-8. Integrond progrom for coupled strip.

-3-12334

```
      FUNCTION TSUM(XN,ARG1)
      IMPLICIT REAL*8 (A-H,O-Z)
      COMMON /FSUB/ DIST(2,100),F,U1,E1,WO,SD,D,XINT,I
      MS=(SD/2.0)/D.D25+1
      MW=(SO/2.0+WD)/D.025
      S=0.0
      M=MS-1
    6 M=M+1
      SIGMA=DIST(I,M)
      ARG3=ARG1*M*0.025
      IF(I.EQ.1) C=DSIN(ARG3)
      IF(I.EQ.2) C=DCDS(ARG3)
      S=S+SIGMA*C
      IF(M.LT.MW) GO TO 6
      TSUM=S
      RETURN
      END
```

Fig.E-9. Fourier transform program for coupled strip.

```
      IMPLICIT REAL*8 (A-H,O-Z)
      COMMON /FSUB/ U1,E1,WD,D,F,XINT
      COMMON /AM/ D1,D2,D3,D4,N1,N2,N3,N4
      DIMENSION TRY(3)
      NAMELIST /NAM1/ U1,E1,W0,D,F,SQ
      CALL CPNMON
      N1=601
      N2=301
      N3=201
      N4=101
      DO 100 JP=1,4
      WRITE(6,31)
   31 FORMAT(' U1,E1,W0,D,F,SQ')
      READ(5,NAM1)
      D1=25./600.
      D2=25./300.
      D3=25./200.
      D4=25./100.
      XINT=SUM(SQ)
      WRITE(6,NAM1)
      WRITE(6,38) SQ,XINT
   38 FORMAT(/' PSI=',E12.5,'  VALUE OF INTEGRAL=',E12.5/)
  100 CONTINUE
   12 CALL EXIT
      END
```

Fig. E-10. General program for Z_o.

-3-12336

```
      FUNCTION FN(XN,SQ)
      IMPLICIT REAL*8 (A-H,O-Z)
      COMMON /FSUB/ U1,E1,WD,D,F,XINT
      IF(XN.EQ.D.D) GO TO 4
      DL=D/3D.
      ARG1=D.2*3.1415927*XN/WD
      ARG3=D.31415927*XN
      P3=193.5D92066/XN**3
      P1=9.5492966B/XN
      P2=6D.7927109/XN**2
      A=1./XN*(P3+(P1-P3)*DCOS(ARG3)+(2.-P2)*DSIN(ARG3))
      T=U1*E1-SQ
      Q=(SQ-1.)/T
      R=(U1*E1-1.)/T
      DTDEF=DTANH(ARG1)
      C1=192./3.1415927*U1/DSQRT(SQ)
      IF(F.EQ.D.D) GO TO 44
      A1=(ARG1/(F*DL))**2
      A2=(2.*3.1415927)**2*T
      SIGN=1.
      B12=(A2-A1)
      IF(B12.LT.D.D) SIGN=-1.
      B1=DSQRT(SIGN*B12)
      Z=DTAN(F*DL*B1)
      IF(B12.LT.D.D) Z=DTANH(F*DL*B1)
      B2=DSQRT((2.*3.1415927)**2*(SQ-1.)+A1)
      PART=SIGN*(Q*U1*Z+SIGN*B2/B1)
      XNUM=C1*R*Q*Z*A/(F*DL*WD*B1)
      XDEN=R**2+SIGN*E1/SQ*B12/A1*PART*(Q/Z-1./E1*B2/B1)
      GO TO 43
   44 PART=Q*U1*DTDEF-1.D
      XNUM=5.D*C1*R*Q/XN*A*DTDEF
      XDEN=R**2-E1/SQ*PART*(Q*1.0/DTDEF-1.0/E1)
   43 IF(XDEN.EQ.0.D) WRITE(6,42) XNUM,XDEN
   42 FORMAT(' NUM=',E12.5,' DEN=',E12.5)
      FN=XNUM/XDEN
      GO TO 5
    4 FN=D.D
    5 RETURN
      END
```

Fig.E-11. Integrand program for Z_o.

V. MODIFICATION FOR MICROSTRIP HAVING A DEMAGNETIZED FERRITE SUBSTRATE

All the programs given in the previous sections of this appendix may be used for obtaining $\xi = \mu_{eff}\epsilon_{eff}$ and Z_o of demagnetized ferrite microstrip if the following minor revisions are made:

(a) The ferrite's saturation magnetization, symbolized by "SATM," is an additional input parameter. Thus, it must be added to all "COMMON" statements, the "NAMELIST" statement, and statement 31.

(b) In the integrand program, the following statements must be inserted between the fourth and fifth lines:

```
SATMN = 2.8*SATM/F
U1 = 2./3.*(1.-SATMN**2)**0.5+1./3.
```

The output of this program will be $\xi = \mu_{eff}\epsilon_{eff}$.

VI. MODIFICATION FOR COUPLED MICROSTRIP ON MAGNETIZED FERRITE SUBSTRATE WITH FIELDS CIRCULARLY POLARIZED

The following minor revisions of the coupled strip program in Sec. III must be made when the substrate material is magnetized ferrite and the RF magnetic fields are circularly polarized.

(a) The ferrite's saturation magnetization and remanence ratio, denoted by the symbols SATM and RR, respectively, are additional input parameters. They must be added to all "COMMON" statements, the "NAMELIST" statement, and statement 31.

(b) In the integrand program, the following statements must be inserted between the fourth and fifth lines:

```
SATMN = 2.8*SATM/F
UMIN = DSQRT(1.-SATMN**2)
U1 = UMIN+(1.-UMIN)*RR**2-SATMN*RR
```

The output of this program is $\xi = \mu_{eff}\epsilon_{eff}$.

ACKNOWLEDGMENT

I wish to express my gratitude to Dr. Nabil Farhat for his very helpful supervision and to my associates at M. I. T. Lincoln Laboratory for their varied and generous support.

REFERENCES

1. F. Assadourian and E. Rimai, "Simplified Theory of Microstrip Transmission Systems," Proc. IRE 40, 1651-1657 (December 1962).
2. G. Deschamps, "Theoretical Aspects of Microstrip Waveguides," Abstract, Trans. IRE MTT-2 (1), 100-102 (April 1954).
3. M. Schetzen, "Printed Microwave Systems," M. S. Thesis, Dept. of Electrical Engineering, M. I. T. (1954).
4. K. G. Black and T. J. Higgins, "Rigorous Determination of the Parameters of Microstrip Transmission Lines," Trans. IRE MTT-3, 93-113 (March 1955).
5. T. T. Wu, "Theory of the Microstrip," J. Appl. Phys. 28 (3), 299-302 (March 1957).
6. M. E. Brodwin, "Propagation in Ferrite-Filled Microstrip," Trans. IRE MTT-6 (2), 150-155 (April 1958).
7. A. A. Van Trier, "Guided Electromagnetic Waves in Anisotropic Media," Appl. Sci. Res. B-3, 305-371 (December 1953).
8. H. A. Wheeler, "Transmission-Line Properties of Parallel Wide Strips by a Conformal-Mapping Approximation," Trans. IEEE MTT-12, 280-289 (May 1964).
9. _____, "Transmission-Line Properties of Parallel Strips Separated by a Dielectric Sheet," Trans. IEEE MTT-13 (2), 172-185 (March 1965).
10. H. E. Green, "The Numerical Solution of Some Important Transmission Line Problems," Trans. IEEE MTT-13 (5), 676-692 (September 1965).
11. M. Caulton, J. J. Hughes, and H. Sobol, "Measurements on the Properties of Microstrip Transmission Lines for Microwave Integrated Circuits," RCA Review 27 (3), 377-391 (September 1966).
12. P. Silvester, "TEM Wave Properties of Microstrip Transmission Lines," Proc. IEE (London) 115 (1), 43-48 (January 1968).
13. E. Yamashita and R. Mittra, "Variational Method for the Analysis of Microstrip Lines," Trans. IEEE MTT-16 (4), 251-256 (April 1968).
14. E. Yamashita, "Variational Method for the Analysis of Microstrip-Like Transmission Lines," Trans. IEEE MTT-16 (8), 529-535 (August 1968).
15. C. P. Hartwig, D. Massé, and R. A. Pucel, "Frequency Dependent Behavior of Microstrip," 1968 IEEE G-MTT International Symposium Digest, 110-116.
16. T. G. Bryant and J. A. Weiss, "Parameters of Microstrip Transmission Lines and of Coupled Pairs of Microstrip Lines," Trans. IEEE MTT-16 (12), 1021-1027 (December 1968).
17. H. E. Stinehelfer, Sr., "An Accurate Calculation of Uniform Microstrip Transmission Lines," Trans. IEEE MTT-16 (7), 439-444 (July 1968).
18. G. I. Zysman and D. Varon, "Wave Propagation in Microstrip Transmission Lines," 1969 IEEE G-MTT International Symposium Digest, 3-9.
19. J. D. Welch, M. I. T. Lincoln Laboratory, private communication.
20. J. Brown, "The Types of Waves Which May Exist Near a Guiding Structure," Proc. IEE (London) 100, Part III, 363-364 (November 1953).
21. R. E. Collin, Field Theory of Guided Waves (McGraw-Hill, New York, 1960), pp. 10, 170-174, 483-485.
22. D. W. Kammler, "Calculation of Characteristic Admittances and Coupling Coefficients for Strip Transmission Lines," Trans. IEEE MTT-16 (11), 929 (November 1968).
23. J. C. Maxwell, A Treatise on Electricity and Magnetism (Dover, New York, 1954), 3rd ed., Vol. 1, p. 296-297.
24. J. A. Stratton, Electromagnetic Theory (McGraw-Hill, New York, 1941), pp. 349-351.
25. E. Denlinger, "Radiation from Microstrip Resonators," Trans. IEEE MTT-17 (4), 235-236 (April 1969).
26. E. Hellman and J. Palocz, "The Effect of Neighboring Conductors on the Currents and Fields in Plane Parallel Transmission Lines," Trans. IEEE MTT-17 (5), 254-259 (May 1969).

27. H. Hair and G. T. Roome, "Thin Ferrite Devices for Microwave Integrated Circuits," Trans. IEEE MTT-16 (7), 411-420 (July 1968).

28. A. G. Gurevich, Ferrites at Microwave Frequencies (Consultants' Bureau, New York, 1963), Chap. V.

29. R. S. Mueller and F. J. Rosenbaum, "Electromagnetic Wave Propagation Along a Ferrite Loaded Wire," Trans. IEEE MTT-17 (2), 92-100 (February 1969).

30. _____, "Propagation in Ferrite-Filled Coaxial Transmission Lines," Trans. IEEE MTT-16 (10), 835-842 (October 1968).

31. D. Kelley, A. Kramer, and F. Willwerth, "Microstrip Filters and Couplers," Trans. IEEE MTT-16 (8), 560-562 (August 1968).

32. P. N. Butcher, "On the Coupling Impedance of Tape Structures," L'One Electrique 37, No. 367, 863-877 (October 1957).

33. W. Libbey, "Theory of Nonreciprocal Active Networks," Ph. D. Dissertation, Dept. of Electrical Engineering, Worcester Polytechnic Institute (1968).

34. E. Jones and J. Bolljahn, "Coupled Strip Transmission Line Filters and Directional Couplers," Trans. IRE MTT-4, 75-81 (April 1956).

35. D. Polder, "On the Theory of Ferromagnetic Resonance," Phil. Mag. 40, 99 (1949).

36. E. Schlömann, J. Green, F. Sandy, and J. Saunders, "Characterization of the Microwave Tensor Permeability of Partially Magnetized Materials," Technical Report 69-93, RADC (February 1969), pp. 33-71.

37. P. Troughton, "Measurement Techniques in Microstrip," Electronics Letters 5 (2), 25-26 (January 1969).

38. W. E. Courtney, private communication.

39. R. E. Collin, Foundations for Microwave Engineering (McGraw-Hill, New York, 1966), pp. 174-177.

DOCUMENT CONTROL DATA – R&D

(Security classification of title, body of abstract and indexing annotetion must be entered when the overall report is classified)

1. ORIGINATING ACTIVITY *(Corporate author)* Lincoln Laboratory, M.I.T.	2a. REPORT SECURITY CLASSIFICATION Unclassified 2b. GROUP None

3. REPORT TITLE

Dynamic Solutions for Single and Coupled Microstrip Lines

4. DESCRIPTIVE NOTES *(Type of report and inclusive detes)*

Technical Report

5. AUTHOR(S) *(Lest name, first name, initial)*

Denlinger, Edgar J.

6. REPORT DATE 19 November 1969	7a. TOTAL NO. OF PAGES 80	7b. NO. OF REFS 39
8a. CONTRACT OR GRANT NO. AF 19(628)-5167 b. PROJECT NO. 7X263304D215 c. d.	9a. ORIGINATOR'S REPORT NUMBER(S) Technical Report 470. 9b. OTHER REPORT NO(S) *(Any other numbers that may be assigned this report)* ESD-TR-69-338	

10. AVAILABILITY/LIMITATION NOTICES

This document has been approved for public release and sale; its distribution is unlimited.

11. SUPPLEMENTARY NOTES None	12. SPONSORING MILITARY ACTIVITY Office of the Chief of Research and Development, Department of the Army

13. ABSTRACT

This investigation presents theoretical and experimental results of single and coupled microstrip propagation on both a pure dielectric and a ferrite substrate. The theory enables one to obtain the frequency dependence of phase velocity and characteristic impedance and also to obtain the electromagnetic field quantities around the microstrip line. It utilizes a Fourier transform method in which the hybrid mode solutions for a "fictitious" surface current at the substrate-air interface are summed in such a way as to represent the fields caused by a current distribution that is finite only over the region occupied by the conducting strip and is assumed equal to that for the static case. The theory for the magnetized ferrite microstrip takes into account both the diagonal and off-diagonal components of the substrate's permeability tensor.

Excellent agreement is obtained between experimental and theoretical results for single microstrip lines on both ceramic and demagnetized ferrite substrates. Coupled line experimental data also agree well with theory and show a significant difference in the amount of dispersion of the two normal modes of propagation, the even mode and the odd mode.

The coupled microstrip theory is then applied to two commonly used microwave integrated circuit devices, the directional coupler and the meander-line phase shifter. Since the even- and odd-mode phase velocities for ferrite-filled coupled lines are closer together than those for the pure dielectric case, the coupler performance with ferrite is shown to be significantly better than with ceramic. Theoretical results which illustrate the nonreciprocal character of the meander-line's propagation constants are also presented.

14. KEY WORDS

frequency dispersion
single microstrip lines
coupled microstrip lines
ferrite substrate
dielectric substrate
microstrip transmission lines
microwave energy propagation
microwave integrated circuits
directional coupler
Fourier transform method